

---

## **Creep of metal matrix composites reinforced by combining nano-sized dispersoids with micro-sized ceramic particulates or whiskers (review)**

---

L. M. Peng\* and S. J. Zhu<sup>†‡</sup>

\*Japan Fine Ceramics Center, Mutsuno 2-4-1, Atsuta-ku, Nagoya 456-8587, Japan

<sup>†</sup>Institute of Industrial Science, The University of Tokyo, Komaba 4-6-1, Meguro-ku, Tokyo, 153-8505, Japan

<sup>‡</sup>Corresponding author: E-mail: zhu@iis.u-tokyo.ac.jp

**Abstract:** The micro-sized ceramic whiskers or particulates can greatly increase the specific modulus and other mechanical properties of aluminium alloys. However, the strength at high temperatures depends on microstructures of the matrix. The nano-sized fine dispersoids can markedly increase the high temperature strength of aluminium alloys, but elastic modulus of these dispersion-strengthened alloys is not significantly improved. Therefore, a new kind of metal matrix composite reinforced by combining nano-sized dispersoids with micro-sized ceramic whisker- or particulate-reinforcements, has been developed. This paper presents the experimental results and analysis on the effects of micro-sized ceramic whiskers or particulates on creep strain rates in the composites by taking account into the load transfer model from matrix to reinforcements. In particular, comparison of creep behavior between titanium and aluminium matrix composites is conducted. Technological barriers and trends associated with practical utilization, development and research of metal matrix composites are also addressed.

**Keywords:** Creep, dispersion-strengthening, load transfer, metal matrix composite, threshold stress.

**Reference** to this paper should be made as follows: Peng, L. M. and Zhu, S. J. (2003) 'Creep of metal matrix composites reinforced by combining nano-sized dispersoids with micro-sized ceramic particulates or whiskers (review)', *Int. J. of Materials & Product Technology, Special Issue – Microstructure and Mechanical Properties of Progressive Composite Materials*, Vol. 18, Nos 1/2/3, pp. 215–254.

---

### **1 Introduction**

The particulate- or whisker-reinforced metal matrix composites (MMCs) are of interest because they can be fabricated through conventional metal processing technique and exhibit near-isotropic properties [1–20]. The composites are being considered for structural and functional applications at elevated temperatures.

Therefore, an understanding of their high-temperature behavior, i.e., creep deformation, is important.

The investigations on creep of discontinuously reinforced MMCs were carried out in the 1980s. The anomalous creep behavior of aluminium matrix composites, that is, the unusually high apparent stress exponent and apparent activation energy for creep, was attractive since they were inconsistent with the existing theoretical or phenomenological models for dislocation creep [9–34]. Most investigators made their analysis of creep data by incorporating a threshold stress into the power-law creep expression to get the true stress exponent and activation energy for creep [9–34]. Park *et al.*'s study [16,17] showed that the threshold stress introduced by the presence of SiC particulate was much lower than the experimental value. Therefore, they suggested an alternative source for the threshold stress was associated with the detachment of dislocations from fine oxide dispersoids, formed as a result of processing the composites by powder metallurgy. However, the temperature dependence of detachment stress is much weaker than that of experimental threshold stress. Mohamed *et al.* [17] proposed that the detachment process might be affected by impurity segregation at the matrix/incoherent dispersoid interfaces. Cadek *et al.* [22] proposed that the creep mechanism of MMCs was lattice-diffusion-controlled dislocation creep in aluminium matrix. Further research demonstrated that creep of MMCs was controlled by creep mechanisms of the matrix alloys [23–30]. The effects of the micro-sized reinforcements on creep were interpreted by a load transfer model, although there have been contradictory arguments on the contributions [24].

On the other hand, limited experimental data on creep behavior of particulate or whisker reinforced titanium matrix composites showed that the stress exponent and activation energy for creep of MMCs were similar to those of the matrix alloys [1–8]. This is quite different from the results observed in aluminium matrix composites. Furthermore, it did not hold true in the case of titanium matrix composites, where either strengthening or weakening was reported [35, 36]. This implies that the micro-sized reinforcements are not very effective to increase creep resistance and the microstructure of the matrix is important for controlling creep deformation of MMCs.

The objectives of the present article are threefold: (1) to show creep behavior in a new kind of metal matrix composite reinforced by combining nano-sized dispersoids with micro-sized ceramic whisker- or particulate-reinforcements; (2) to understand the contributions of nano-sized dispersoids on creep resistance in micro-sized ceramic whisker- or particulate-reinforced MMCs; and (3) to demonstrate the role played by the micro-sized ceramic reinforcements in the creep deformation of composites.

## **2 Creep of discontinuous titanium matrix composites**

The prohibitive cost of continuous fibers, complex fabrication routes and highly anisotropic properties of continuously reinforced titanium matrix composites have motivated the development of discontinuously reinforced composite. Among the alternative discontinuous reinforcements, TiC and TiB<sub>2</sub> particulates or whiskers are particularly attractive due to their complete compatibility with titanium and its alloys. The most widely used matrices are designed to contain both  $\alpha$  and  $\beta$  phases to

provide the highest combination of strength and ductility. As a result, Ti-6Al-4V, which contains both  $\alpha$  and  $\beta$  stabilizers is chosen as matrix since it exhibits good fluidity, excellent weldability, good tensile strength and ductility [37]. In this section, the limited experimental data and analysis for creep deformation in TiC and/or TiB<sub>2</sub> reinforced titanium matrix composites will be presented.

Zhu *et al.* [1–3, 7] studied the creep deformation of 15 vol.% TiCp/Ti-6Al-4V (TiCp stands for TiC particulate) and 15 vol.% TiB<sub>2</sub>w/Ti-6Al-4V (TiB<sub>2</sub>w stands for TiB<sub>2</sub> whisker) composites between 823 and 923 K in both tension and compression conditions. The composites were fabricated by a powder metallurgy technique. Figures 1(a) and (b) show the microstructure of Ti-6Al-4V alloy and 15 vol.% TiCp/Ti-6Al-4V, respectively. It is seen that the microstructure of matrix is refined by TiC particulates with inhomogeneous distribution throughout the matrix.

The variation of steady-state creep rate,  $\dot{\epsilon}$ , with applied stress,  $\sigma$ , is shown in Figure 2 for these two composites together with Ti-6Al-4V alloy at different temperatures ranging from 823 to 923 K [1–3, 7]. The steady-state creep rate can be described through an Arrhenius-type equation of the form

$$\dot{\epsilon} = \frac{ADGb}{kT} \left( \frac{\sigma}{G} \right)^n, \quad (1)$$

where  $n$  is the apparent stress exponent,  $D$  ( $= D_0 \exp(-Q/RT)$ ,  $D_0$  is a frequency factor) the diffusion coefficient,  $Q$  the apparent activation energy for creep,  $G$  the shear modulus,  $b$  the Burgers vector,  $k$  the Boltzmann's constant,  $A$  a dimensionless constant, and  $T$  the absolute temperature. The compressive (solid circle) and tensile (empty circle) data points at 873 K fall quite close to each other, which implies that the flow behavior of the 15 vol.% TiCp/Ti-6Al-4V composite exhibits no tension/compression asymmetry. It is obvious that the presence of TiC particulates and TiB<sub>2</sub> whiskers is quite effective in improving the creep resistance of the matrix. The former decreases creep rate of the matrix alloy by one order of magnitude and the latter by about two orders of magnitude at a given testing temperature, i.e., 873 K. The data indicate that there are two distinct regimes (designated as regions I and II) depending on the applied stress. It can be noted that the stress exponent for creep deformation increases with an increase in the applied stress at the three testing temperatures. For instance, the stress exponent changes from 3~4 in region I to 7~9 in region II for the titanium matrix alloy and its composites.

The recent investigations of Ranganath and Mishra [4, 6] on Ti, Ti-Ti<sub>2</sub>C, and Ti-TiB-Ti<sub>2</sub>C composites reveal that the creep rate decreased with increasing volume fractions of reinforcement and that the creep rate of the composites were 2~3 orders of magnitude lower than the unreinforced Ti in the temperature range of 823~923 K. Furthermore, the creep strengthening is more significant in the case of high volume fraction of reinforcement. It was also observed that the stress exponents of the composites were between 6~7 at 823 K (in case of higher volume fraction of reinforcements, i.e., 0.15 and 0.25) but similar to unreinforced Ti ( $n = 4.1 \sim 4.3$ ) at higher temperatures, i.e., 873 and 923 K. For unreinforced Ti and 10 vol.% TiB + Ti<sub>2</sub>C composite,  $n$  seems to be independent of temperature. This implies that the stress dependence of the composites depends on both the volume fraction of reinforcements and testing temperature.

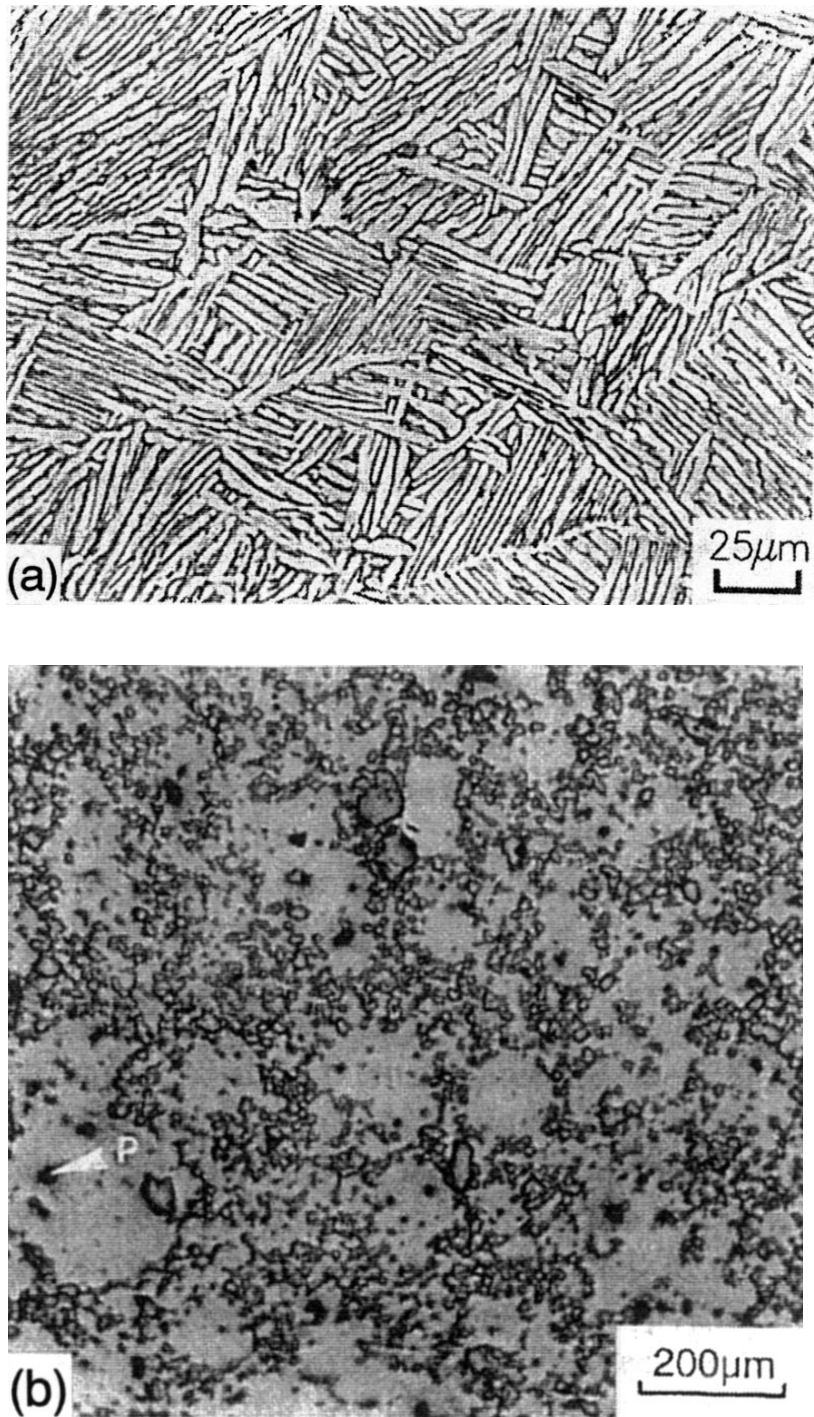


**Figure 1** Microstructures of (a) a standard Ti-6Al-4V alloy in the  $\beta$  phase region and (b) the composite showing the underlying microstructural details of the matrix [7].

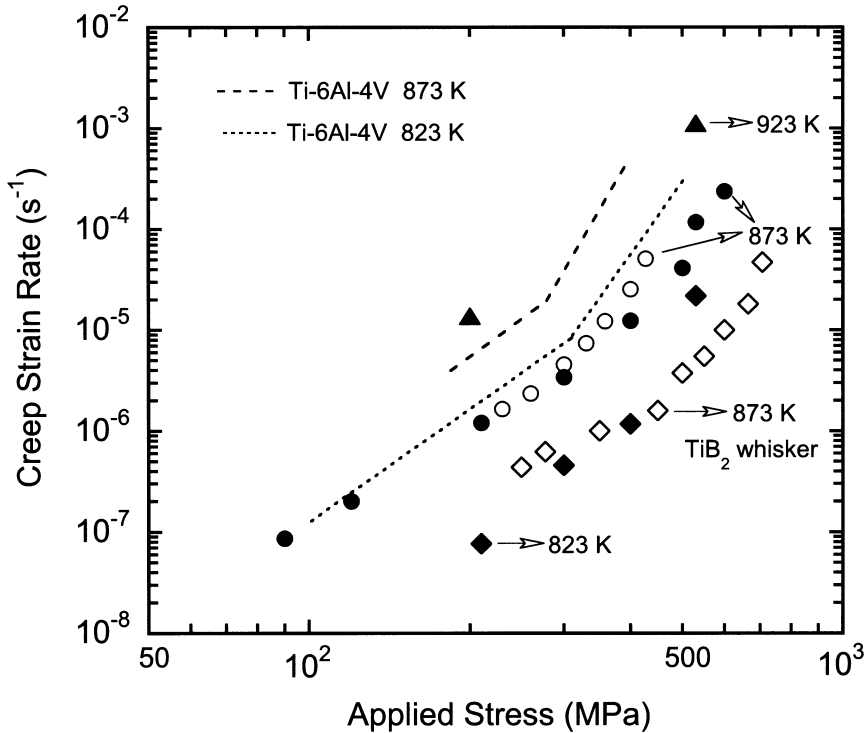
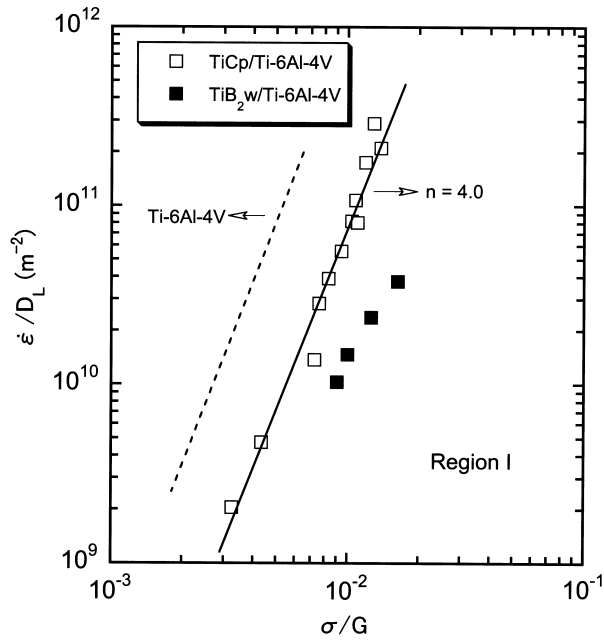


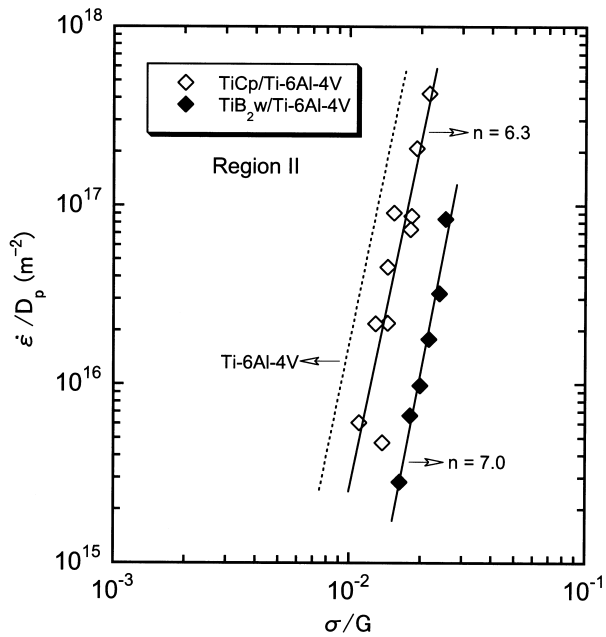
**Figure 2** A comparison of the creep rate between  $\text{TiCp}/\text{Ti-6Al-4V}$  and  $\text{TiB}_2\text{w}/\text{Ti-6Al-4V}$  composites under tensile (open symbols) and compressive (solid symbols) conditions at 823, 873, and 923 K.

On the other hand, the above results show that the effect of reinforcements on the stress exponent of Ti matrix composites is quite different from the trends observed in aluminium matrix composites. As will be demonstrated in Section 3, the stress exponent for creep in aluminium matrix composites is 15 or above and the activation energy much higher than the anticipated value for lattice self-diffusion in pure aluminium ( $142 \text{ kJ mol}^{-1}$ ) is often observed. It is documented that the change of stress exponent of composites with stress, temperature and volume fraction of reinforcements is due to a change in the creep mechanism from lattice-diffusion controlled dislocation climb ( $n = 4.3$ ) to pipe-diffusion controlled dislocation climb ( $n = 7$ ) [4].

Since the diffusion (self- or pipe-) coefficient in the h.c.p.  $\alpha$ -Ti is much lower than that in b.c.c.  $\beta$ -Ti [38], the diffusion in  $\alpha$ -Ti should be the rate-controlling process for creep in  $\alpha + \beta$  alloys. Therefore, in Equation (1) the  $D$  and  $G$  values corresponding to  $\alpha$ -Ti are to be employed to analyze the data. Taking  $G [\text{MPa}] = 4.95 \times 10^4 - 25T$  [39], lattice self-diffusion  $D_L [\text{m}^2 \text{s}^{-1}] = 1.3 \times 10^{-2} \exp(-242,000/RT)$ , and pipe-diffusion  $D_p = 3.6 \times 10^{-16} \exp(-97,000/RT)$  for  $\alpha$ -Ti [38], the relations between the creep rate normalized by corresponding diffusion coefficient and applied stress normalized by shear modulus are shown in Figure 3(a) and (b) for Zhu *et al.*'s original creep data, respectively. There are two points worth noting. Firstly, the creep data in both region I and II can be reconciled so that all of the experimental datum



(a)



(b)

**Figure 3** A comparison of the normalized creep data of  $\alpha$ -Ti with those of TiCp/Ti-6Al-4V and TiB<sub>2</sub>w/Ti-6Al-4V composites for low stress exponent regime (Region I) and (b) high stress exponent regime (Region II).

points fall onto a single line in a normalized plot. The stress exponent in region I for TiCp/Ti-6Al-4V composite is 4.0, very close to that ( $n = 4.3$ ) for power-law creep controlled by lattice self-diffusion in  $\alpha$ -Ti whereas it is less than 4.0 for TiB<sub>2</sub>w/Ti-6Al-4V due to the limited data. In region II it is 6.3 and 7.0 for these two composites, respectively. Again, they are close to the value for creep where the pipe-diffusion process is the operative mechanism in  $\alpha$ -Ti. Secondly, the creep strengthening effects of reinforcements arise again on these normalized plots. Moreover, at a given volume fraction of reinforcement, the whisker composite exhibits superior creep resistance to particulate composite (c.f. Figure 3(a) and (b)). It is also apparent that at high stresses or strain rates, strengthening by particulates or whiskers is less effective, which may be attributed to the debonding between reinforcement/matrix interface or fracture of reinforcements.

It is supposed that there exist two possibilities responsible for the creep strengthening of composites without a change in the stress exponent value [4, 6, 7]. The first possibility is the presence of load transfer from the matrix to the stiffer particulates and/or whiskers. From Eq. (1) it is clear that an increase in the modulus of composites yields lower creep rate [1]. The other possibility originates from microstructural strengthening in composites [7]. The addition of reinforcements to titanium alloy leads to a refined  $\alpha + \beta$  colony microstructure as compared to the unreinforced titanium [7]. It is well known that  $\alpha + \beta$  morphology has a very strong effect on the strength properties in titanium alloys [40]. In this case, the dislocation generation and annihilation can easily occur at the  $\alpha/\beta$  boundaries, which also serve as barriers to dislocation slip. As for the effect of volume fraction, Ranganath *et al.* [4, 6] suggest that a modification in the dimensionless constant,  $A = 3.2 \times 10^5 \exp(-24.2V_f)$  for the lattice diffusion region and  $A = 4.4 \times 10^5 \exp(-28.1V_f)$  (where  $V_f$  is the volume fraction of reinforcements) for the pipe-diffusion region to take the influence of reinforcements into account on the creep kinetics. As a result, it was established that the high creep strength of composites is achieved through combined effects of an increased modulus of the composites and the refined microstructure.

### 3 Creep of dispersion-strengthened aluminium matrix composites

Large improvements in high temperature performance, i.e., creep resistance of metallic materials especially aluminium alloys can be achieved by the formation of non-shearable, nano-sized (usually dispersoid radius  $< 100$  nm as dislocation theory required) dispersoids exhibiting chemical stability and low coarsening tendency. Dispersoid strengthening in metals results from dispersoids impeding the motion of matrix dislocations within the grains or at grain boundaries [41–44]. However, the moduli of these dispersion-strengthened (DS) aluminium alloys are not markedly improved. A promising approach to achieve this objective is to combine nanometer-scale dispersoids and micro-sized ceramic reinforcements. The latter strengthening rests on the load transfer from the soft matrix onto the hard reinforcements. As a result, a new family of materials—dispersion-strengthened aluminium matrix composites has been developed with superior performance such as higher specific modulus, higher specific strength and higher creep resistance than the corresponding

monolithic alloy [45–56]. They are now being considered for high temperature applications. Therefore, the creep behavior of these metal matrix composites (MMCs) has attracted considerable interest in recent years.

Despite different size scales, there are still some fundamental similarities in creep behavior between DS matrix alloys and their discontinuously reinforced composites by ceramic particulates or whiskers. Their creep behavior is often characterized by exceptionally high and variable values for the apparent stress exponent  $n_a (= [\partial \ln \dot{\epsilon} / \partial \ln \sigma]_T$ , where  $\dot{\epsilon}$  is the creep rate and  $\sigma$  is the applied stress) and the apparent activation energy  $Q_a (= [R \partial \ln \dot{\epsilon} / \partial (1/T)]_\sigma$ , where  $R$  is the universal gas constant and  $T$  is the absolute temperature).

In order to assess the potential of these advanced composites for use as structural materials for high temperature application, it is necessary not only to systematically investigate the creep properties of these composites but also to conduct a close comparison between the creep behavior of a composite and that of its unreinforced matrix alloy under similar experimental conditions. As a consequence, the objective of the present section is to examine whether the incorporation of ceramic whiskers (SiC,  $\text{Al}_{18}\text{B}_4\text{O}_{33}$  and  $\text{Si}_3\text{N}_4$ ) or particulates (SiC) into DS alloys (PM Al-Fe-V-Si and MA Al-C) results in a strengthening effect and to identify the role of the reinforcements and the matrix alloy during the creep of the composites. Moreover, some other relevant fundamental aspects with respect to the creep deformation will also be addressed.

### 3.1 Creep in PM Al-8.5Fe-1.3V-1.7Si MMCs reinforced by whiskers

Detailed creep experiments were carried out by Peng *et al.* [48–51] on PM Al-8.5Fe-1.3V-1.7Si (wt.%, denoted Al-Fe-V-Si in the following) alloy and its several composites over the temperature range from 573 to 823 K. They are reinforced with 15 vol.% of SiC,  $\text{Al}_{18}\text{B}_4\text{O}_{33}$  and  $\text{Si}_3\text{N}_4$  whiskers, respectively (hereafter denoted as SiCw/Al-Fe-V-Si,  $\text{Al}_{18}\text{B}_4\text{O}_{33}\text{w}/\text{Al-Fe-V-Si}$  and  $\text{Si}_3\text{N}_4\text{w}/\text{Al-Fe-V-Si}$ ). The details regarding to fabrication of the composites and experimental descriptions can be found elsewhere [48–51]. From several previous investigations [44, 46, 47, 57–59], the microstructure of PM Al-Fe-V-Si consists of very fine grain size (about 0.4  $\mu\text{m}$ ) and small and round dispersoids. The vast majority of dispersoids have the composition of  $\text{Al}_{12}(\text{Fe},\text{V})_3\text{Si}$  phase with an average radius of 47 nm, which are homogeneously distributed throughout the aluminium matrix. The dispersoids made up a volume fraction of about 0.27 and were found to be thermally stable. The representative microstructure of SiCw/Al-Fe-V-Si composite is illustrated in Figure 4. The  $\text{Al}_{18}\text{B}_4\text{O}_{33}\text{w}/\text{Al-Fe-V-Si}$  and  $\text{Si}_3\text{N}_4\text{w}/\text{Al-Fe-V-Si}$  composites had the similar microstructure. It can be found that the dispersoids and whiskers are aligned along the extrusion direction. The aspect ratio of SiC whiskers is reduced from 100 (before extrusion processing) to 10 by processing.

A logarithmic plot of the steady-state creep rate,  $\dot{\epsilon}$  vs the applied stress,  $\sigma$ , is shown in Figure 5 for (a) the unreinforced Al-Fe-V-Si alloy and (b) the SiCw/Al-Fe-V-Si composite. Inspection of the creep data for both materials demonstrates that the steady-state creep rate can be related to stress and temperature through Eq. (1). As can be seen in the figures, the datum points for any temperature and any composite can be approximated by a straight line, whose slope is defined as the apparent stress

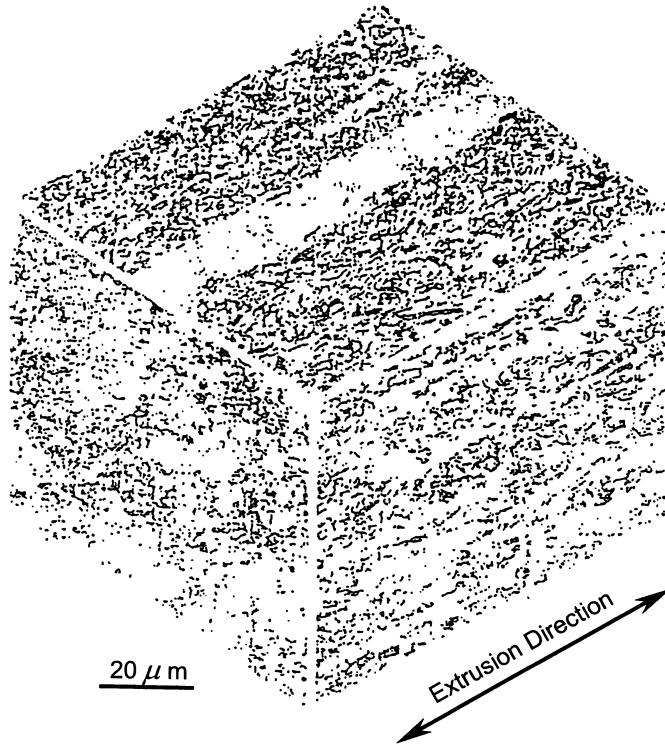
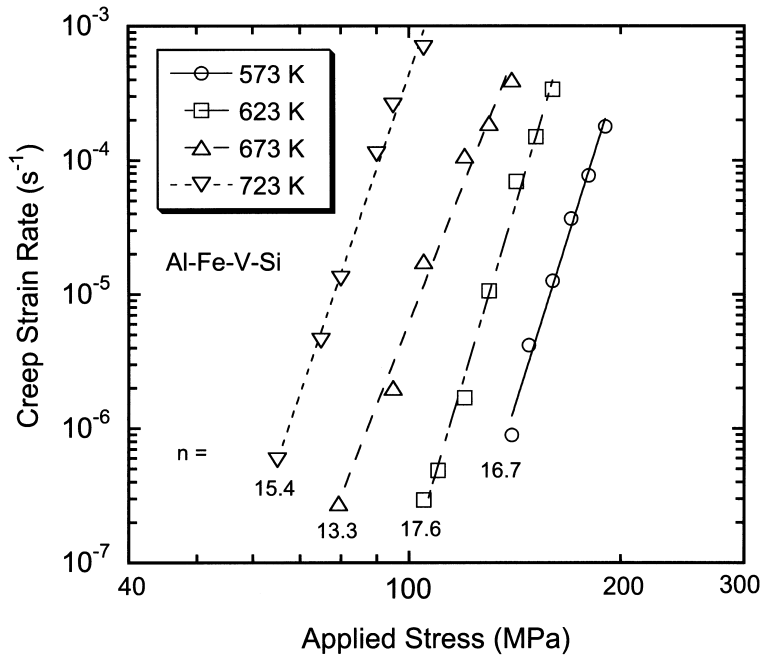


**Figure 4** Microstructure of SiCw/Al-Fe-V-Si composite [48].

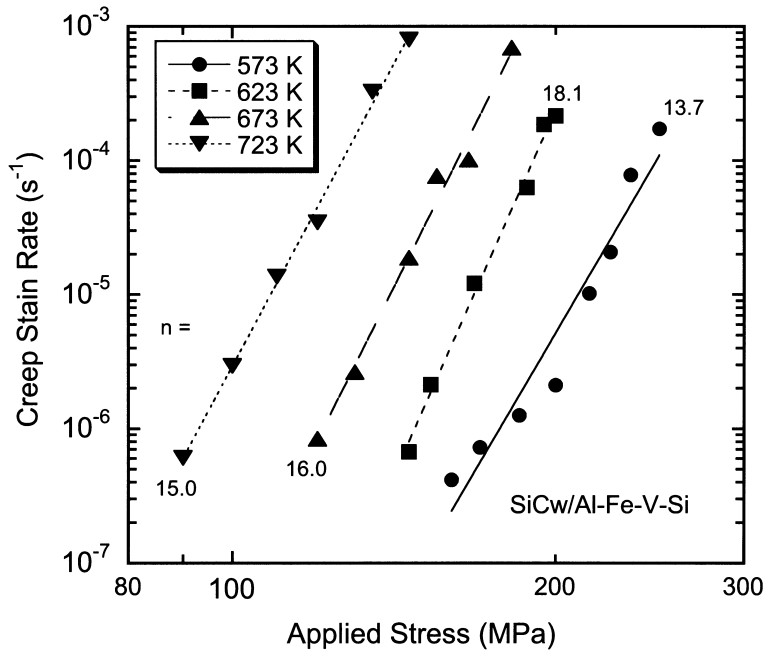
exponent,  $n_a$ . The present results differ from those of other investigations on PM 2124 and 6061 Al alloy [60, 61] and their SiC reinforced aluminium composites [24, 26] where  $n_a$  is variable with the applied stress, i.e., increasing with decreasing the applied stress. One possibility responsible for this discrepancy is that the present creep data are obtained only over four orders of magnitude ( $10^{-7}$ – $10^{-4}$  s $^{-1}$ ) instead of  $10^{-9}$ – $10^{-2}$  s $^{-1}$  available in other investigations [26, 60, 61]. Owing to the very strong stress dependence of creep rate, it is difficult to estimate the apparent activation energy of creep,  $Q_a$ . However,  $Q_a$  can be estimated by using the data of Figure 5 and by the following equation

$$Q_a = -R \left[ \frac{\ln(\dot{\epsilon}_1/\dot{\epsilon}_2)}{(1/T_1 - 1/T_2)} \right]_{\sigma} \quad (2)$$

The values of  $n_a$  and  $Q_a$  for Al-Fe-V-Si and its composites are summarized in Table 1. For both Al-Fe-V-Si matrix alloy and its whisker reinforced composites, the values of apparent stress exponent,  $n_a$ , and the apparent activation energy,  $Q_a$ , vary with testing temperature and applied stress, respectively. These values lie within the range of  $n_a = 11$ – $18.1$  and  $Q_a = 195$ – $395$  kJ mol $^{-1}$ , respectively. They are very high by comparison with the stress exponents of  $n = 3$ – $5$  reported for the creep of pure Al or traditional solid solution Al alloys and with the anticipated activation energy for creep which should be close to the value for self-diffusion in Al (142 kJ mol $^{-1}$ ) or for



(a)



(b)

**Figure 5** Steady-state or minimum creep rate vs applied stress for (a) the Al-Fe-V-Si alloy and (b) SiCw/Al-Fe-V-Si composite.

**Table 1** Summary of creep investigations on Al-Fe-V-Si and its composites reinforced by whiskers ( $Q_a^{\text{exp}}$  in kJ mol<sup>-1</sup> and  $\sigma$  in MPa).

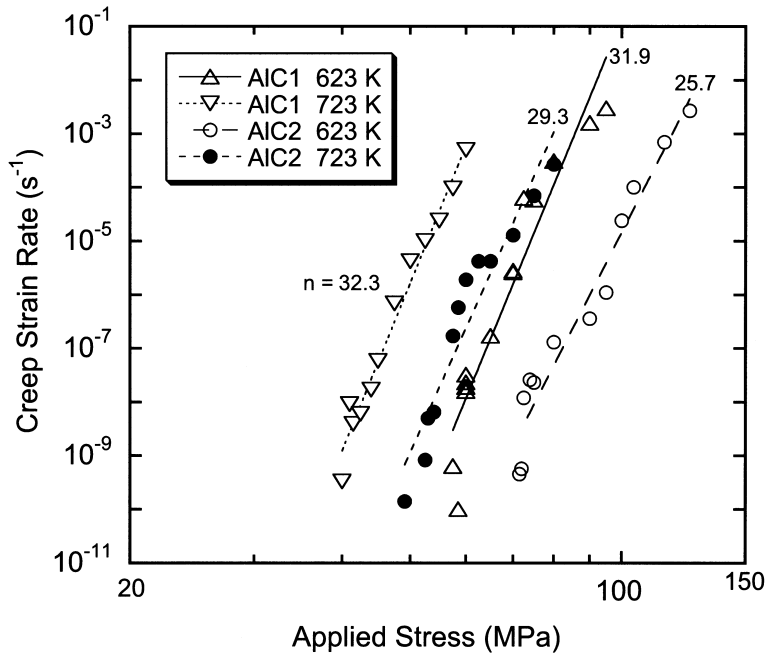
$T$ (K)	Al-Fe-V-Si			SiCw/ Al-Fe-V-Si			Al <sub>18</sub> B <sub>4</sub> O <sub>33</sub> W/ Al-Fe-V-Si			Si <sub>3</sub> N <sub>4</sub> W/ Al-Fe-V-Si	
	$n_a$	$Q_a^{\text{exp}}$	$Q_a^{\text{calc}}$	$n_a$	$Q_a^{\text{exp}}$	$Q_a^{\text{calc}}$	$n_a$	$Q_a^{\text{exp}}$	$Q_a^{\text{calc}}$	$n_a$	$Q_a^{\text{exp}}$
573	16.7	195	200	13.7	264	293	12.6	240			227
623	17.6	( $\sigma=160$ )	( $\sigma=160$ ,	18.1	( $\sigma=146$ )	( $\sigma=146$ ,	14.1	( $\sigma=200$ )			( $\sigma=80$ )
673	13.3	296	$T=673$ K)	16.0	303	$T=623$ K)		236	246		336
723	15.4	( $\sigma=105$ )	278	15.0	( $\sigma=120$ )	270	13.5	( $\sigma=129$ )	( $\sigma=129$ ,		( $\sigma=60$ )
773		395	( $\sigma=105$ ,			( $\sigma=120$ ,			$T=723$ K)	12.3	
823		( $\sigma=95$ )	$T=673$ K)			$T=723$ K)					11.0

interdiffusion of relevant solute atoms, i.e., Mg in the Al lattice (i.e., 130 kJ mol<sup>-1</sup> for Mg in Al [25]). In general, the incorporation of ceramic whiskers into DS Al-Fe-V-Si alloy does not evidently influence either the stress or temperature dependence of the creep rates of the matrix alloy. This is different from the effects of SiC whiskers or particulates on the creep behavior of pure aluminium or traditional aluminium alloy matrix composites [18, 19]. However, it is consistent with the results on the creep behavior of SiC whiskers reinforced PM 6061 Al composites [24] or SiC particulates reinforced PM 2124 Al composites [26], where the matrix alloy contains oxide dispersoids generated due to the P/M route.

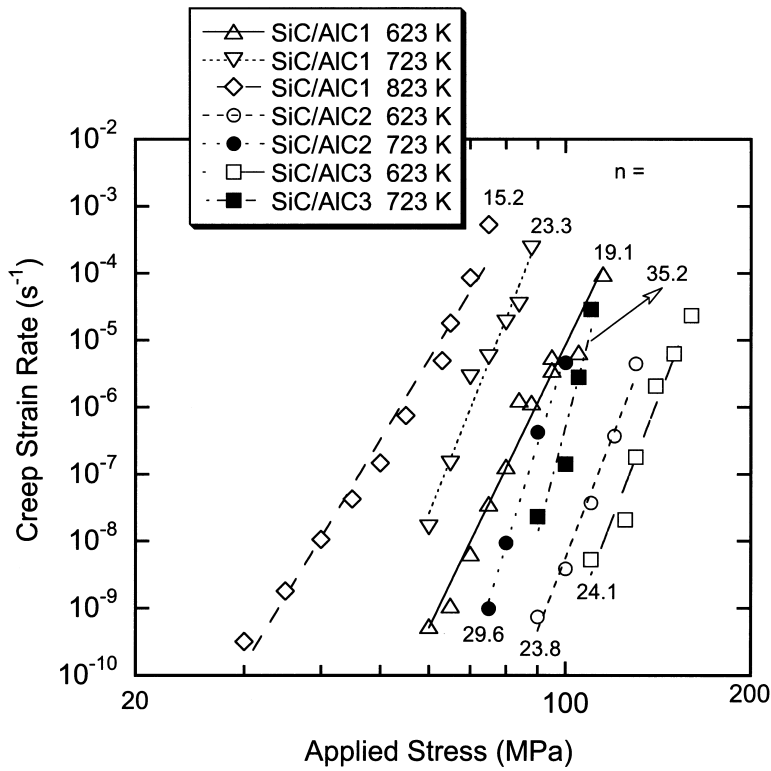
### 3.2 Creep in MA Al-C MMCs reinforced by SiC particulates

Recently, mechanical alloying technique has been extensively applied to fabricate another class of advanced metal matrix composites, among which the matrix alloys were strengthened by fine and stable aluminium carbide, Al<sub>4</sub>C<sub>3</sub> and alumina, Al<sub>2</sub>O<sub>3</sub> [52, 53]. Experiments were conducted to determine the creep properties of Al-SiCp/Al<sub>4</sub>C<sub>3</sub> composites. The volume fraction of SiC particulates with an average diameter of 10  $\mu\text{m}$  was fixed to 10 vol.%, the volume fraction of Al<sub>4</sub>C<sub>3</sub> dispersoids was defined by the content of carbon in the Al-C matrix alloys. Therefore, SiC/AlC $X$  ( $X = 1, 2$  and 3) denotes the Al-C alloy reinforced by 10 vol.% SiC particulates;  $X$  wt.% carbon was added to the aluminium powder before the mechanical alloying. A more detailed description of the material processing and creep tests can be found in Refs [52, 53].

The steady-state (minimum) creep rate is plotted as a function of stress for DS Al-C matrix alloy in Figure 6(a) and for SiC/AlC composites in Figure 6(b). Using the power-law equation to describe the stress dependence of the creep rate, the apparent stress exponents range from  $n_a = 25.7$  to  $n_a = 32.3$  for the DS Al-C alloys and from  $n_a = 15.2$  to  $n_a = 35.2$  for the SiC/AlC composites. It can be found that at any given temperature, the exponent  $n_a$  for the SiC/AlC composites increases with the volume fraction of aluminium carbide dispersoids. At the same time, the value of  $n_a$  at 723 K is higher than at 623 K. Also, the creep resistance of both Al-C alloys and SiC/AlC composites increases with increasing volume fraction of Al<sub>4</sub>C<sub>3</sub> dispersoids at the same applied stress. The apparent activation energy,  $Q_a$  for creep is estimated on the



(a)



(b)

**Figure 6** Steady-state or minimum creep rate vs applied stress for (a) the AIC1 and AIC2 alloys and (b) the SiC/AICX ( $X = 1, 2$  and 3) composites.

basis of Eq. (2), with a value ranging from 286 to 446 kJ mol<sup>-1</sup> for Al-C alloys and from 200 to 322 kJ mol<sup>-1</sup> for composites, respectively. Again, these materials exhibit anomalous creep characteristics as have been described in the Al-Fe-V-Si system materials.

In order to eliminate the influence of temperature on creep rate and compare the strengthening effect of different ceramic reinforcements, Figures 7 and 8 show the relations between  $\dot{\epsilon}/D_L$  and  $\sigma/G$  for the two systems of DS aluminium alloys and their composites, where  $D_L$  ( $= 1.71 \times 10^{-4} \exp(-142.12/RT)$  [m<sup>2</sup> s<sup>-1</sup>] [62]) and  $G$  ( $= 3.0 \times 10^4 - 16T$  [MPa] [63]) are the coefficient of self-diffusion and shear modulus of pure aluminium, respectively. Inspection of these figures reveals the following features. Firstly, the datum points of each material at different temperatures can be represented by a single line with a slope of still more than 10 or collapse within a narrow band. This implies that creep deformation of all the materials may be controlled by lattice diffusion of aluminium. Secondly, at any given value of normalized stress,  $\sigma/G$ , the normalized creep rate,  $\dot{\epsilon}/D_L$  in the composites reinforced either by ceramic whiskers or particulates are more than two and three orders of magnitude lower than those in their matrix alloy—Al-Fe-V-Si and Al-C, respectively.

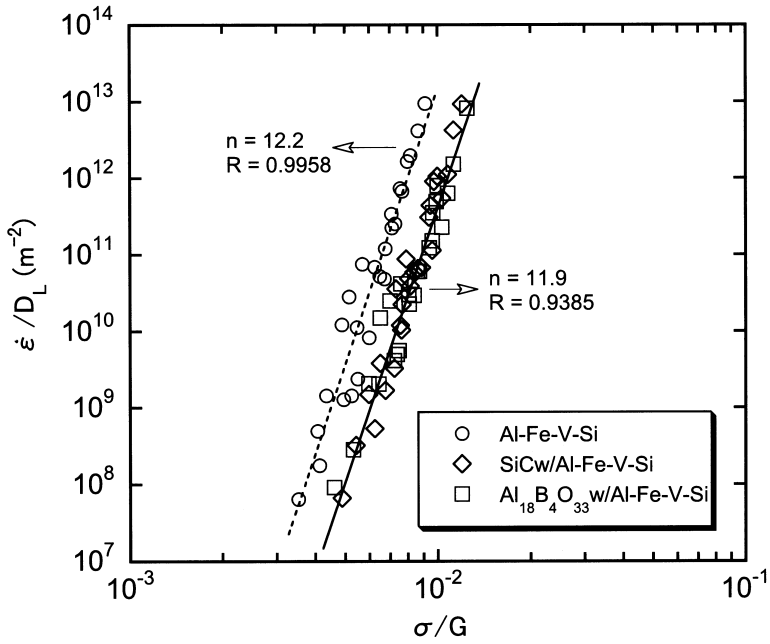
The parallel curves of the matrix alloy and the composites suggest the possibility of the occurrence of load transfer during the creep of composites, which will be addressed in the succeeding part. However, there are two points worth noting. Firstly, when the Si<sub>3</sub>N<sub>4</sub>/Al-Fe-V-Si composite is tested at the temperature higher than 773 K, the creep strengthening effect of whisker diminishes before a threshold stress is incorporated into the analysis (c.f. Figure 7(b)). Secondly, for the SiC/AlC1 composite, the normalized creep curve exhibits concave-upward shape and the stress exponent increases with increasing normalized stress when the creep test is carried out at 823 K (c.f. Figure 8(d)).

### 3.3 Interpretation of the creep data using a threshold stress

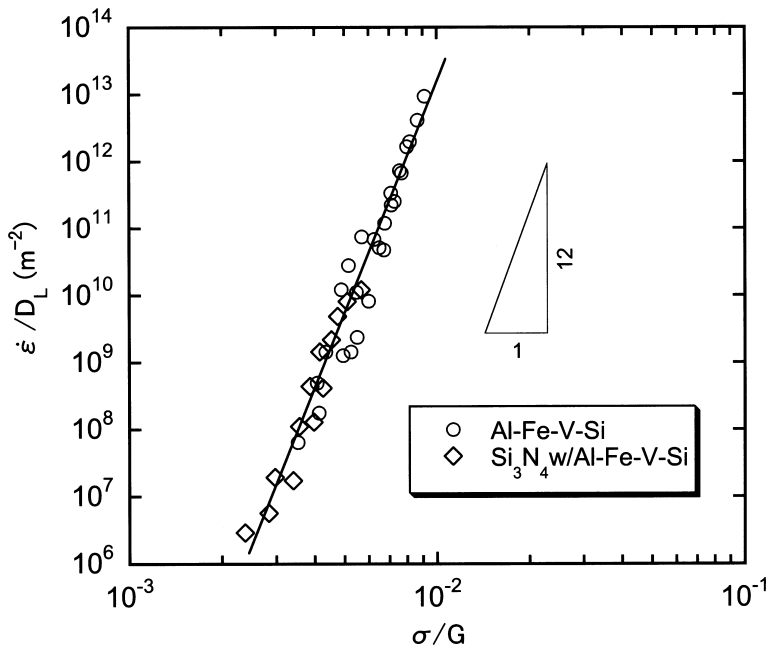
As stated previously, the creep behavior of dispersion strengthened PM Al-Fe-V-Si, MA Al-C alloys and their composites, unlike that of pure Al or solid solution strengthened Al alloys, cannot be described by the simple power-law creep Eq. (1). However, the anomalous stress dependence of creep rate in these materials suggests that it is appropriate to incorporate a threshold stress,  $\sigma_{th}$ , into the simple power-law equation; the observed creep deformation is driven by an effective stress  $\sigma_e (= \sigma - \sigma_{th})$  instead of the applied stress,  $\sigma$ . In this case, the creep behavior is controlled by a rate equation of the form

$$\dot{\epsilon} = \frac{ADGb}{kT} \left( \frac{\sigma - \sigma_{th}}{G} \right)^n \quad (3)$$

Then, these high values for  $n_a$  and  $Q_a$  will be reduced to lower and constant values for the true stress exponent and the true activation energy, and these lower values are usually close to those anticipated from creep of pure metals and solid-solution alloys. Accordingly, it is appropriate to examine the rate-controlling mechanisms in the creep of MMCs based on the well-established creep processes for metals and alloys. On the other hand, it is usual to anticipate that the value of the

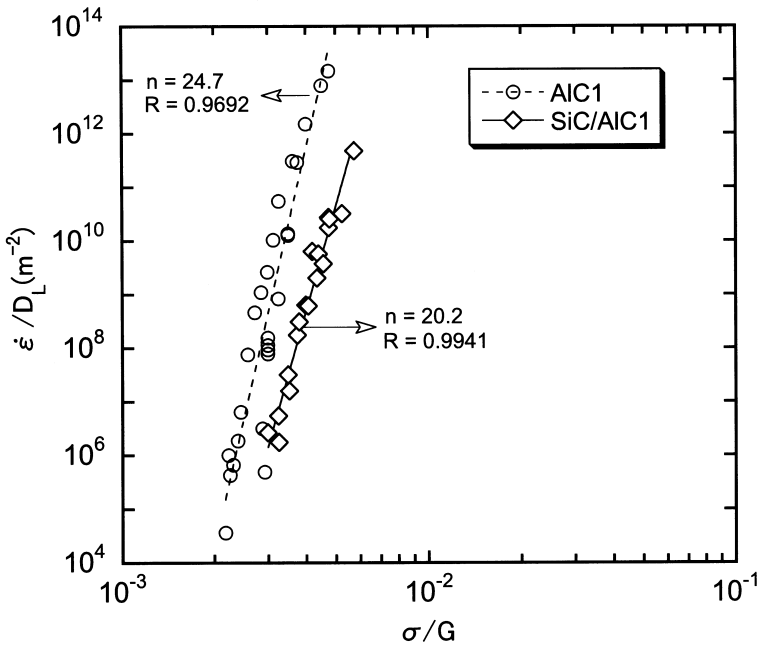
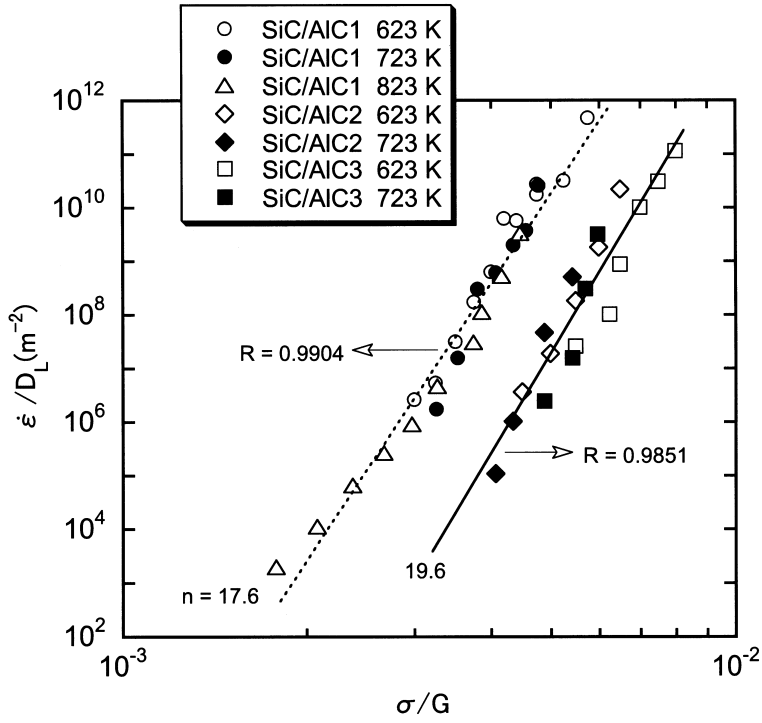


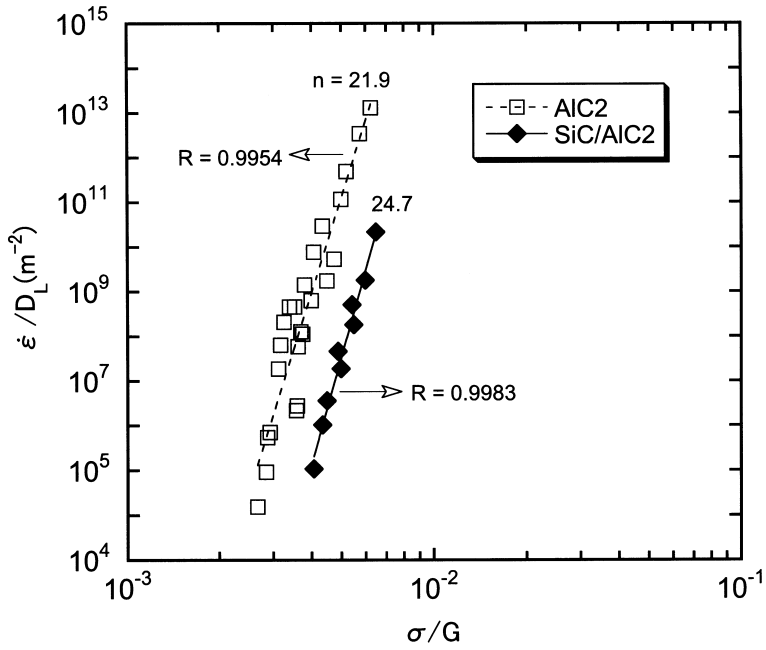
(a)



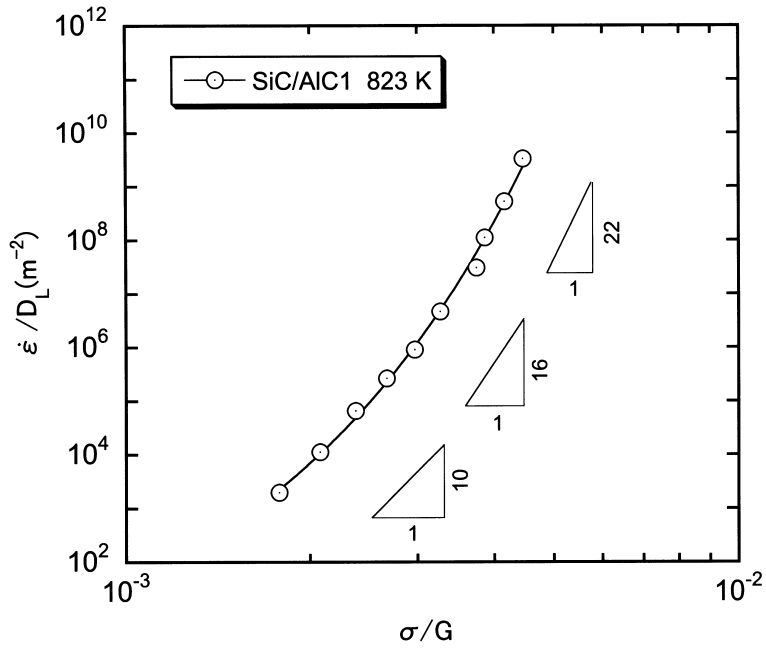
(b)

**Figure 7** Diffusion-compensated strain-rate vs modulus-compensated stress for (a) Al-Fe-V-Si, SiCw/Al-Fe-V-Si and Al<sub>18</sub>B<sub>4</sub>O<sub>33</sub>w/Al-Fe-V-Si and (b) Si<sub>3</sub>N<sub>4</sub>w/Al-Fe-V-Si. A value of 142 kJ mol<sup>-1</sup> was used for the activation energy.





(c)



(d)

**Figure 8** Diffusion-compensated strain-rate vs modulus-compensated stress for (a) AlC1 and SiC/AlC1, (b) AlC2 and SiC/AlC2, (c) SiC/AlCX ( $X = 1, 2$  and 3), and (d) SiC/AlC1 at 823 K. A value of  $142 \text{ kJ mol}^{-1}$  was used for the activation energy.

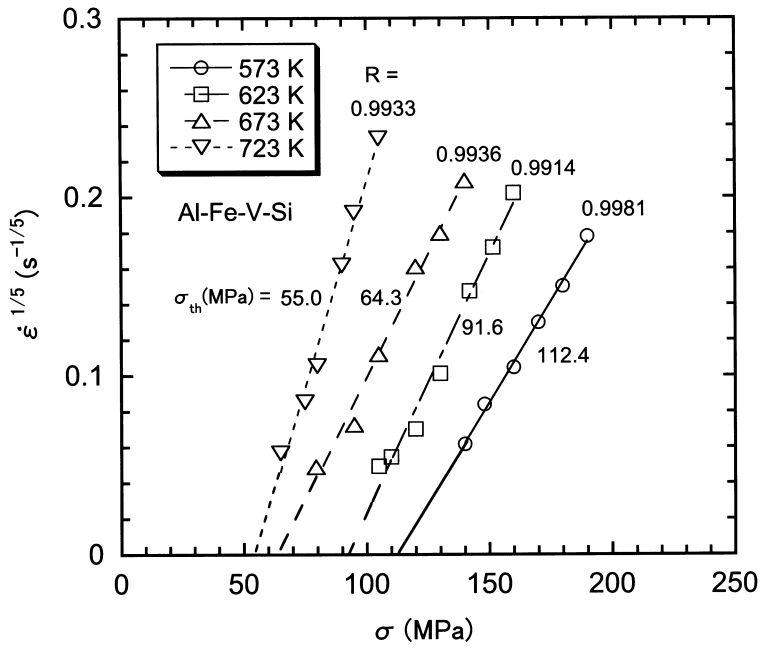
true stress exponent,  $n$  will take values of 3, 5, or 8, representing the viscous glide of dislocations [64, 65], high temperature climb of dislocations [66], or a constant substructure model [67], respectively. When  $n = 3$ , the anticipated activation energy is close to the value for the interdiffusion energy of solute atoms, whereas when  $n = 5$  or  $n = 8$ , the anticipated activation energy is close to the value for lattice self-diffusion in the crystalline.

The standard procedure in determining the most appropriate value for the true stress exponent is to replot the  $\log \dot{\epsilon}$  vs  $\log \sigma$  data onto a linear-scale diagram of  $\dot{\epsilon}^{1/n}$  vs  $\sigma$  using different values of  $n$  and then to select the value of  $n$  giving the best linear fit to the datum points [24, 49–56]. At the same time, the straight fitting line's intersection with the horizontal axis of zero strain rate provides the value of  $\sigma_{th}$ .

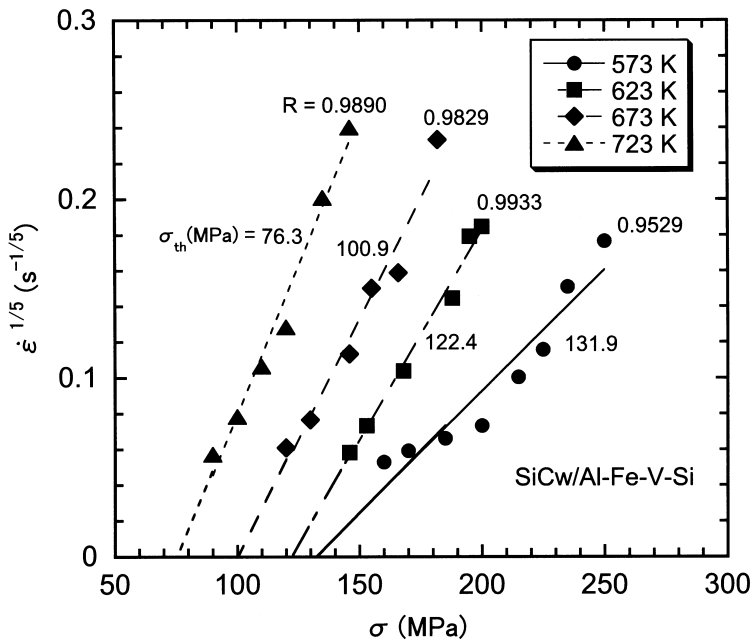
Thus, in Figure 9,  $\dot{\epsilon}^{1/5}$  is plotted against  $\sigma$  in double linear coordinates for Al-Fe-V-Si alloy and SiCw/Al-Fe-V-Si composites on the basis of analysis of creep data for the matrix alloy. Using the third power of creep rate, the curves exhibit an upward-curvature, and do not fit the linear relationship. Simultaneously, the supersaturation of Fe, V, and Si in the Al matrix has been reported to be around 0.5 pct, 0.1 pct, and 0.1 pct, respectively [57]. Therefore, viscous glide is unlikely to control the creep of Al-Fe-V-Si alloy and its composites because the high volume fraction of stable intermetallic dispersoids  $Al_{12}(Fe,V)_3Si$  leads to a severe depletion in the level of alloying elements in solid solution. Using the eighth power, the curves are linear, but it should be noted that the present data cover only four orders of magnitude. Park *et al.* [16] and Cadek *et al.* [22, 23] found that the eighth power exhibit downward-curvature curves provided the creep rates in aluminium and aluminium alloys reinforced by SiC particulates and/or whiskers cover more than five orders of magnitude. Moreover, a value of  $n = 5$  is consistent with published creep data both for pure Al and, at least over limited ranges of stress, for Al-Mg and Al-Cu solid solution alloys.

Taking the values for  $\sigma_{th}$  listed in Table 2, logarithmic plots of the creep rate vs the effective stress,  $(\sigma - \sigma_{th})$  are presented in Figure 10 for (a) SiCw/Al-Fe-V-Si and (b)  $Al_{18}B_4O_{33}w$ /Al-Fe-V-Si composites. It can be seen that all of the datum points fit well to a series of nearly parallel lines having an average slope of 4.5 and 4.4 for these two composites, respectively. This, in turn, supports the assumed value of the true stress exponent  $n$  close to 5 rather than close to 3 or 8.

Since the true stress exponent for creep in Al-Fe-V-Si and its whiskers reinforced composites is equal to 5, it is reasonable to conclude that creep of these materials is controlled by high-temperature dislocation climb (lattice diffusion) of Al matrix. The true activation energy for creep is close to the value for self-diffusion of Al. To confirm the validity of this conclusion, Figure 11 shows a logarithmic plot of the normalized creep rate,  $\dot{\epsilon}/D_L$ , against the normalized effective stress,  $(\sigma - \sigma_{th})/G$ . It is apparent that all the datum points of both matrix alloy and composites are now brought on or very close to their own line with a slope of  $\sim 5$ . This figure also indicates that even after normalizing the data with the threshold stress and modulus, the normalized creep rate of the whiskers reinforced composites is still lower than that of the matrix alloy, by a factor of  $\sim 60$ . Furthermore, unlike the results as shown in Figure 7(b),  $Si_3N_4$  whiskers exhibit creep strengthening in this figure. Comparatively, the three kinds of whiskers have almost the identical contribution to increasing the creep resistance of matrix alloy. The similar analysis conducted by



(a)



(b)

**Figure 9** The linear extrapolation approach for estimating the threshold stresses using  $n = 5$  for (a) Al-Fe-V-Si and (b) SiCw/Al-Fe-V-Si.

**Table 2** Estimated values for the threshold stress in Al-Fe-V-Si and its composites ( $n = 5$  and  $\sigma_{th}$  in MPa).

$T$ (K)	Al-Fe-V-Si		SiCw/ Al-Fe-V-Si		Al <sub>18</sub> B <sub>4</sub> O <sub>33</sub> W/ Al-Fe-V-Si		Si <sub>3</sub> N <sub>4</sub> W/ Al-Fe-V-Si	
	$\sigma_{th}$	$10^3 (\sigma_{th}/G)$	$\sigma_{th}$	$10^3 (\sigma_{th}/G)$	$\sigma_{th}$	$10^3 (\sigma_{th}/G)$	$\sigma_{th}$	$10^3 (\sigma_{th}/G)$
573	112.4	5.40	131.9	6.33	131.7	6.32		
623	91.6	4.57	122.4	6.11	109.1	5.45		
673	64.3	3.34	100.9	5.25				
723	55.0	2.98	76.3	4.14	67.5	3.66		
773							42.4	2.41
823							32.0	1.90

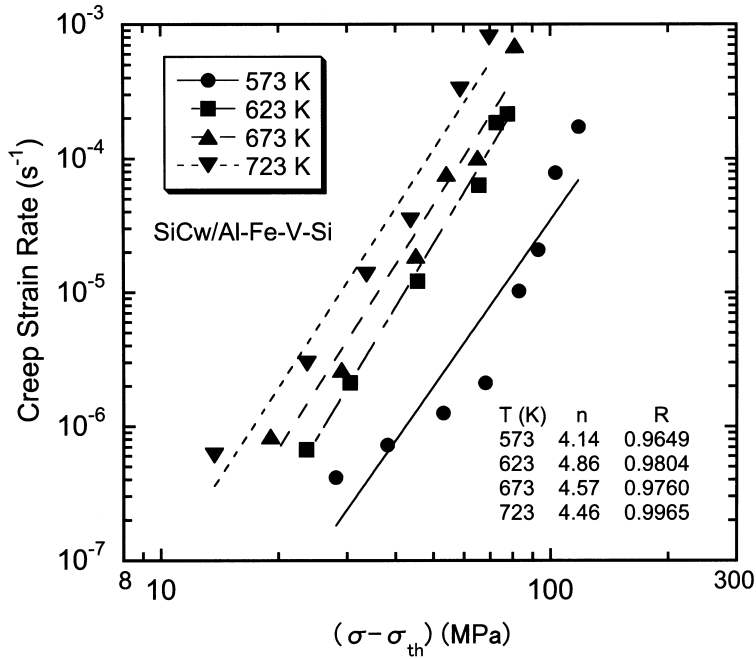
the present authors [52] reveals that the value of  $n = 8$  is preferred to the value of  $n = 5$  at the true stress exponent for Al-C alloys and their composites. Again, at any given selected value of the normalized effective stress,  $(\sigma - \sigma_{th})/G$ , the normalized creep rate,  $\dot{\epsilon}/D_L$  in composites is more than three orders of magnitude lower than that in their corresponding Al-C alloy (Figure 12).

### 3.4 Significance of the threshold stress

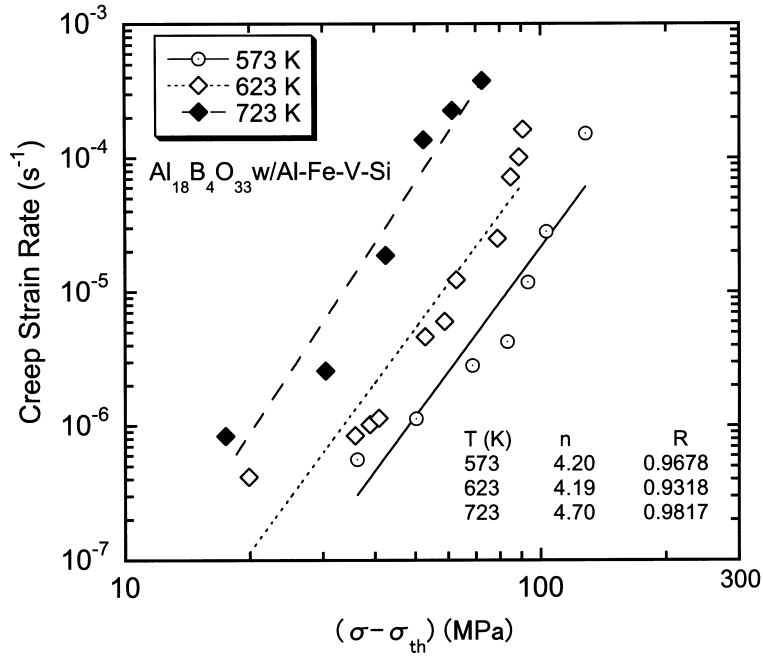
#### 3.4.1 The origin of the threshold stress

The preceding analysis shows that the anomalous stress dependence of creep rates in two systems of DS Al alloys and their composites can be interpreted in terms of a threshold stress. The origin of such a threshold stress is attributed to the presence of fine and stable incoherent dispersoids (Al<sub>12</sub>(Fe,V)<sub>3</sub>Si in DS Al-Fe-V-Si alloy or its composites and Al<sub>4</sub>C<sub>3</sub> in DS Al-C alloys or its composites) which act as effective barriers of dislocation movement. It is reasonably speculated that the ceramic reinforcements are not directly responsible for the threshold stress measured in the composites due to their large size. This is consistent with some other investigators' suggestions [24, 26, 60, 61] that the threshold stress for creep in PM 6061 Al, 2124 Al and their composites is associated with the interactions between moving dislocations and fine oxide dispersoids. These dispersoids form as a result of processing the matrix alloys and composites by powder metallurgy.

For DS alloys, three theoretical deformation models [68–73] that explain the nature of the interaction between incoherent non-shearable dispersoids and dislocations, and give the magnitude of thresholds stresses have been proposed. In these models, the threshold stress is equal to: (a) the stress required to cause dislocation bowing between dispersoids [68, 69] (the Orowan stress),  $\sigma_{Or}$ ; (b) the extra back stress  $\sigma_b$ , required to create an additional segment of dislocation as it surmounts the dispersoid by local climb [70, 71]; and (c) the stress associated with detachment of dislocation from an attractive dispersoid after climb is completed [72, 73]. The expressions of the above threshold stress as well as the characterization of various parameters are summarized in Table 3. The estimated values of  $\sigma_{th}/G$  by substituting the relevant structural parameters into the three threshold stress



(a)



(b)

**Figure 10** Steady-state or minimum creep rate,  $\dot{\epsilon}$  vs effective stress,  $(\sigma - \sigma_{th})$  for (a) SiCw/Al-Fe-V-Si and (b) and  $Al_{18}B_4O_{33}w/Al-Fe-V-Si$ .

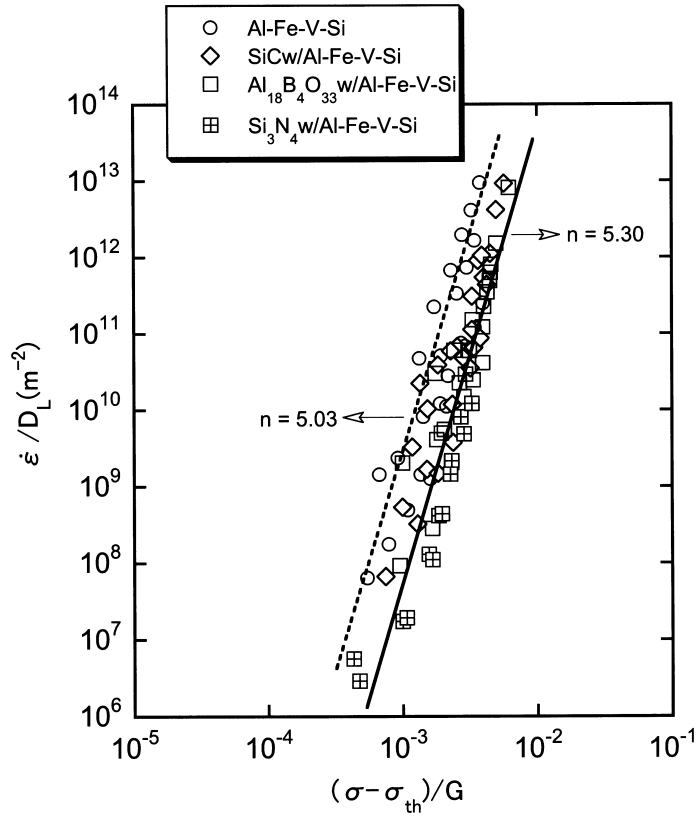


**Figure 11** Normalized creep rate,  $\dot{\epsilon}/D_L$  vs normalized effective stress,  $(\sigma - \sigma_{th})/G$  for Al-Fe-V-Si and whiskers reinforced composites.

equations of Table 3 together with the experimental values for Al-Fe-V-Si and SiCw/Al-Fe-V-Si composite are given in Table 4 and semi-logarithmically plotted in Figure 13 as a function of the reciprocal of the absolute temperature for the purpose of comparison. It can be found that the experimental values follow within the range of  $\sigma_b/G < \sigma_{th}/G < \sigma_d/G$ . Also, the relationships between all the normalized threshold stress data obtained experimentally for the materials under consideration and the reciprocal of the absolute temperature are shown in Figure 14.

### 3.4.2 The temperature dependence of the threshold stress

As evident from Figures 13 and 14, the experimental values of the normalized threshold stress are sensitive to temperature (decreasing with increasing temperature) and such a sensitivity cannot be accounted for by the temperature dependence of the shear modulus. Conversely, the temperature dependence of the predicted threshold stress based on three deformation models arises from the variation of  $G$  with  $T$  since their normalized values,  $\sigma_{th}/G$  are plotted as horizontal lines in Figure 14. Moreover, according to Figures 13 and 14, the variation of experimental  $\sigma_{th}/G$  with  $T$  can be described by the following expression of the Arrhenius form [23, 24, 26, 29, 60, 61]

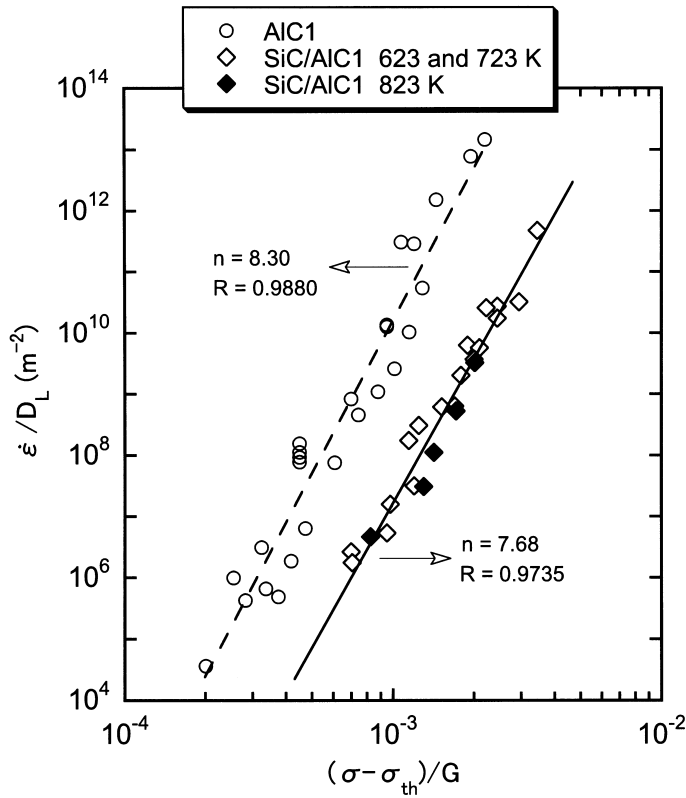


**Figure 12** Normalized creep rate,  $\dot{\epsilon}/D_L$  vs normalized effective stress,  $(\sigma - \sigma_{th})/G$  for AIC1 and SiC/AIC1.

**Table 3** Creep deformation models proposed for the origin of the threshold stress in DS alloys.

Model	Magnitude of $\sigma_{th}/G$	References
Orowan stress	$\sigma_{Or}/G = 0.84Mb \ln(r/b)/[\pi(\lambda - 2r)(1 - \nu)^{1/2}]^*$	[68, 69]
Local climb (back stress)	$\sigma_b/G = 0.3Mb/\lambda$	[70, 71]
Detachment stress	$\sigma_d/G = \sigma_{Or}/G \cdot (1 - k_d^2)^{1/2 \dagger}$	[72, 73]

\* $M$  is the Taylor factor (= inverse of the Schmidt factor of single crystalline materials).

$\dagger k_d$  is a relaxation parameter taking values between 0 (maximum attractive interactions) and 1 (no attractive interactions).

**Table 4** The experimental and estimated values of  $\sigma_{th}/G$  for Al-Fe-V-Si alloy based on the relevant proposed models for dispersoid-dislocation interactions in DS alloys.

$T$ (K)	$10^3 \sigma_{Or}/G$	$10^3 \sigma_b/G$	$10^3 \sigma_d/G$	$10^3 \sigma_{th}/G$ for Al-Fe-V-Si	$10^3 \sigma_{th}/G$ for SiCw/Al-Fe-V-Si
573	46.7	2.36	10.6	5.40	6.33
623	46.7	2.36	10.9	4.57	6.11
673	46.7	2.36	10.8	3.34	5.25
723	46.7	2.36	11.1	2.98	4.14

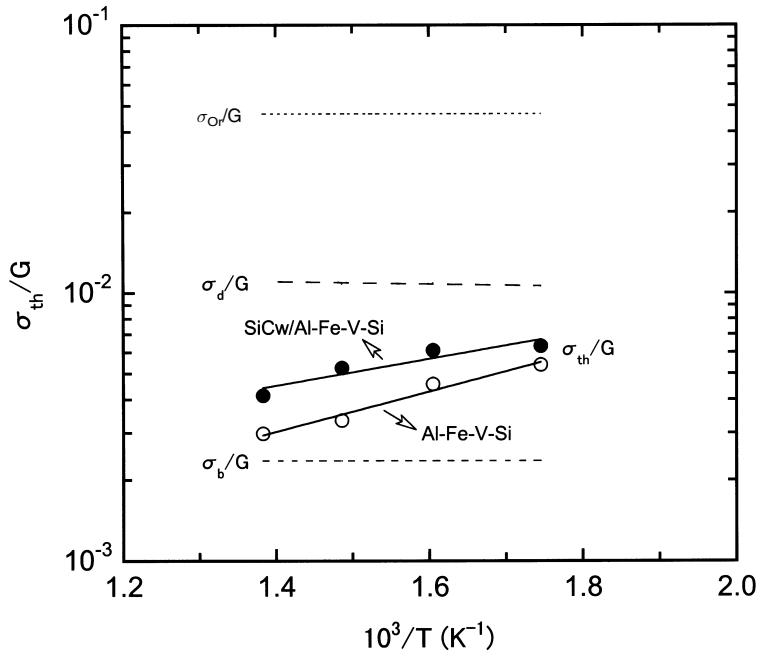


Figure 13 Comparison of magnitude and temperature dependence of normalized experimental and theoretical threshold stress for Al-Fe-V-Si and SiC/Al-Fe-V-Si.

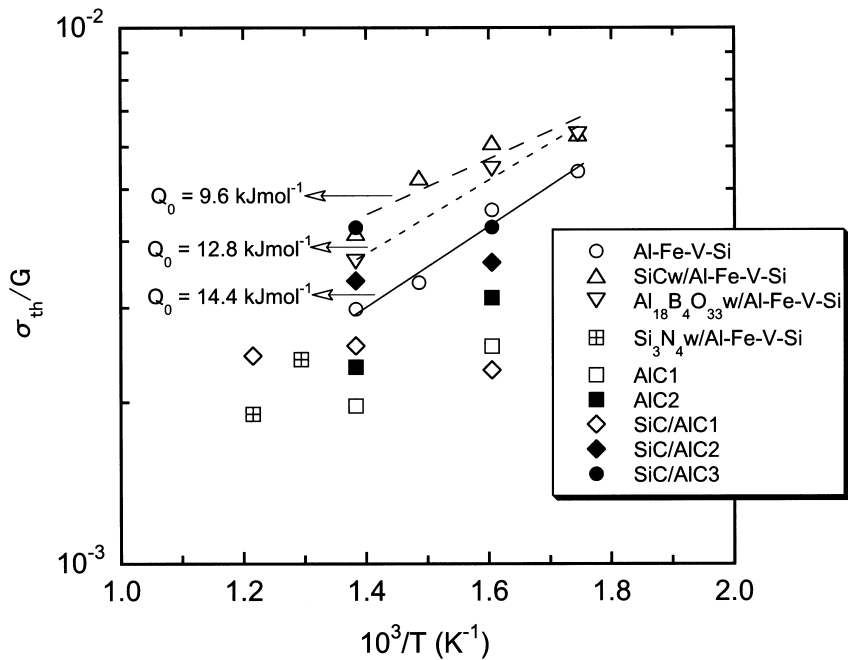


Figure 14 Normalized threshold stress vs reciprocal of absolute testing temperature for all materials under investigations.

$$\frac{\sigma_{\text{th}}}{G} = B_0 \exp\left(\frac{Q_0}{RT}\right), \quad (4)$$

where  $B_0$  is a constant, and  $Q_0$  is an energy. By taking the slope of the straight lines in Figure 14, the estimated values of  $Q_0$  are 14.4, 9.6 and 12.8 kJ mol<sup>-1</sup> for Al-Fe-V-Si alloy, SiCw/Al-Fe-V-Si and Al<sub>18</sub>B<sub>4</sub>O<sub>33</sub>w/Al-Fe-V-Si composites, respectively. Since creep tests were conducted at only two temperatures, it is inappropriate to estimate  $Q_0$  for other materials.

The origin of the strong temperature dependence of the thresholds stress is still not completely clear at the present time. Nevertheless, it is interesting to note that Eq. (4) takes the similar form to that reported for the temperature dependence of  $\sigma_{\text{th}}$  in superplastic materials. For these materials it has been suggested that there is an interaction between impurity atoms segregated at boundaries and dislocations. Thus, a threshold stress proportional to  $\exp(E/RT)$  ( $E$  is the binding energy between an impurity atom and a lattice dislocation with a value of 8.7–26 kJ mol<sup>-1</sup> [74]) is introduced by such an interaction. The estimated values of  $Q_0$  [Eq. (4)] for other DS alloys and some Al matrix composites are summarized in Table 5. There are two main findings worth noting. Firstly, the values of  $Q_0$  is relatively insensitive both to the nature and to the volume fraction of reinforcement in MMCs and similar values of  $Q_0$  are obtained in Al-based alloys without any reinforcements. Secondly, the range of experimental values of  $Q_0$  lies within the reported binding energies between dislocations and impurity atoms in the glide plane [74].

However, some investigations, i.e., on 15 vol.% SiCp/Al-8.5Fe-1.3V-1.7Si [75] or 20 vol.% SiCp/2124Al [76], demonstrated that the true threshold stress creep behavior may disappear above a critical testing temperature when the threshold stress is described by a linear decrease relation with the testing temperature. In this case, a transition occurs from athermally to thermally activated detachment of dislocations from fine dispersoids existing in aluminium matrix of composites [75, 76]. For 20 vol.% SiCp/2124Al composite, the derived critical temperature is 740 K [76]. For the present materials, the critical temperatures are much higher than this value (Figure 15). In particular, for SiCw/Al-Fe-V-Si, the critical temperature is 934 K, which approaches the melting temperature of pure aluminium (933 K [38]).

**Table 5** Estimated values of  $Q_0$  (in kJ mol<sup>-1</sup>) for DS alloys and MMCs based on Eq. (4).

Materials	$Q_0$ (kJ mol <sup>-1</sup> )	References
15 vol.% SiCw/Al-Fe-V-Si	9.6	Present investigation
15 vol.% Al <sub>18</sub> B <sub>4</sub> O <sub>33</sub> w/Al-Fe-V-Si	12.8	Present investigation
PM Al-Fe-V-Si	14.4	Present investigation
PM 2124 Al	27.5	[61]
PM 6061 Al	19.3	[60]
MA 754	10.6	[77]
RS Al-Si-Ni-Cr alloy	21	[78]
30 vol.% SiCp/6061 Al	19.3	[24]
30 vol.% SiC/Al	23	[23]
20 vol.% Al <sub>2</sub> O <sub>3</sub> p/6061Al	25	[15]

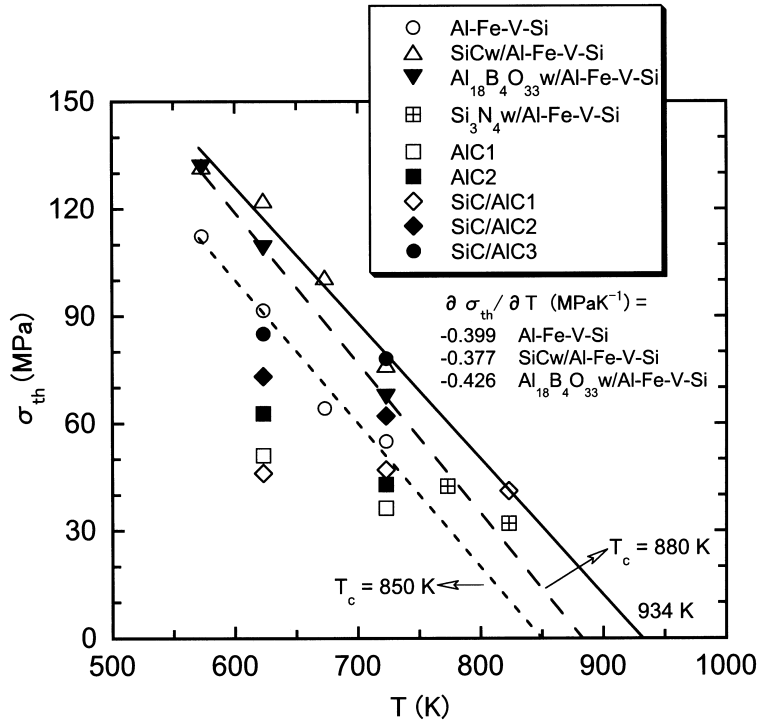


Figure 15 Threshold stress vs absolute testing temperature for all materials to estimate the critical temperature above which the threshold stress diminishes.

One can exclude the possibility that the threshold stress decreases linearly with testing temperatures. Instead, it is more reasonable to use Eq. (4) to describe this relation.

### 3.5 Effect of matrix alloy on creep behavior of MMCs

It is well established that the creep behavior of solid solution alloys is divided into two distinct types, namely class M (metal type) and class A (alloy type) [79]. In the former case, the creep deformation is controlled by dislocation climb with a stress exponent of  $\sim 5$  and an activation energy close to the value for lattice self-diffusion. While in the latter case, the rate-controlling process is viscous glide where dislocation drag solute atoms atmosphere characterized by a stress exponent of  $\sim 3$  and an activation energy related to the interdiffusion of the solute atoms. However, there usually exists a transition from class M to class A behavior under some conditions [80].

Extensive investigations have demonstrated that the creep of MMCs is controlled by the rate of deformation within the matrix alloy. Li *et al.* [28, 29, 32] investigated the creep behavior of 20 vol.% Al<sub>2</sub>O<sub>3</sub> particulates reinforced 6092 Al (Al-1.05Mg-0.83Cu-0.75Si in wt.%) and 7005 Al (Al-4.5Zn-1.0Mg-0.4Fe-0.35Si in wt.%) composites in which Mg and Zn are the major alloying element, respectively. Their results have shown that the former composite exhibits creep behavior of class A type with a true stress exponent of  $\sim 3$  and the same true activation energy as matrix alloy

close to the value of  $\sim 130 \text{ kJ mol}^{-1}$  for creep controlled by viscous glide (or for interdiffusion of Mg in the Al lattice); whereas the creep behavior of the latter composite is characterized by a true stress exponent of  $\sim 4.4$ , which is similar to the value of  $n$  in pure Al, and a true activation energy of  $\sim 120 \text{ kJ mol}^{-1}$ , which is consistent with the value anticipated for lattice self-diffusion in a dilute Al-Zn alloy [28]. Therefore, it is reasonable to conclude that the creep of discontinuously reinforced metal matrix composites is controlled by deformation within the matrix.

For the two systems of materials in the present investigations, the creep behavior of whiskers or particulates reinforced composites is similar to that of their corresponding matrix with regard to: (a) the value of true stress; (b) the value of true activation energy; (c) the interpretation of creep in terms of a threshold stress; and (d) the temperature dependence of the threshold stress as described by Eq. (4). It can be inferred from these similarities in creep behavior between the composites and the unreinforced matrix alloy that deformation in the matrix alloy controls the creep of its composites. Moreover, the origin of the threshold stress for creep in the DS matrix alloy is also responsible for the threshold stress behavior in the composite, which rules out the possibility that ceramic reinforcements (whiskers or particulates) serve directly as a source of  $\sigma_{\text{th}}$ .

### *3.6 Role of ceramic reinforcements*

#### *3.6.1 The magnitude of the threshold stress*

As shown in Figure 14, the values of the threshold stress for creep in the composites are higher than those for their corresponding matrix alloy. There are two possibilities responsible for this discrepancy. Firstly, although the identical procedure is applied to produce the composite and the matrix alloy, the incorporation of hard ceramic reinforcements may exert an effect on the size and distribution of dispersoids in the composites. For instance, the presence of ceramic reinforcements may result in further breaking up of large dispersoids during hot pressing and extrusion process, which in turn could cause a reduction in both the size and spacing of dispersoids in the composites. The second possibility is associated with the fracture of ceramic reinforcements into smaller ones with sizes comparable to those of dispersoids. As a consequence, the volume fraction of dispersion dispersoids could be increased. Therefore, it may be concluded that both the incoherent dispersoids and nanometer-scale ceramic fragments introduced by the extrusion process interact with moving dislocations in the composites.

#### *3.6.2 The role of load transfer*

As demonstrated previously, at any selected normalized (effective) stress, the normalized creep rates in the composites are lower than in their corresponding matrix alloy by  $\sim 2$  or 3 orders of magnitudes, depending on the strengths of matrix in the case of DS Al-C alloys. Therefore, it is evident that the ceramic reinforcements exhibit additional creep strengthening except a contribution to an increase in the magnitudes of threshold stresses. The strengthening mechanism of composite materials based on the load transfer from the matrix to reinforcements was first proposed by Kelly and Street [81]. Their original analysis leads to the following

expression that gives the ratio between the creep rates in the discontinuous fiber reinforced composite and matrix alloy

$$\frac{\dot{\epsilon}_c}{\dot{\epsilon}_m} = \left[ \alpha \left( \frac{L}{d} \right)^{\frac{n+1}{n}} V_f + (1 - V_f) \right]^{-n}, \tag{6}$$

where  $\dot{\epsilon}_c$  is the composite creep rate,  $\dot{\epsilon}_m$  the matrix creep rate at the same temperature and stress,  $L/d$  the aspect ratio of the reinforcement,  $V_f$  the volume fraction of the reinforcement,  $n$  the stress exponent, and  $\alpha$  the load transfer coefficient determined by

$$\alpha = \left( \frac{2}{3} \right)^{\frac{1}{n}} \left( \frac{n}{2n+1} \right) \left[ \left( \frac{2\sqrt{3}}{\pi} V_f \right)^{-\frac{1}{2}} - 1 \right]^{-\frac{1}{n}}. \tag{7}$$

For the whiskers reinforced Al-Fe-V-Si composites, taking  $V_f = 0.15$ ,  $L/d = 10$  and the apparent stress exponent at respective testing temperature, Eq. (7) yields the values of load transfer coefficient for each composite as shown in Table 6 with an average value of 0.461, 0.455 and 0.448 for SiC, Al<sub>18</sub>B<sub>4</sub>O<sub>33</sub> and Si<sub>3</sub>N<sub>4</sub> whiskers reinforced Al-Fe-V-Si composites, respectively. It follows from Eq. (7) that the load transfer coefficient is dependent only on the stress exponent at a given volume fraction of reinforcements. Therefore, it is almost constant when the stress exponent does not vary markedly with the testing temperature. Incorporation of the relevant value of  $\alpha$  into Eq. (6) leads to the average ratio of  $\dot{\epsilon}_c/\dot{\epsilon}_m$  as  $3.82 \times 10^{-4}$ ,  $1.12 \times 10^{-3}$  and  $2.56 \times 10^{-3}$  for the three composites, respectively. It is evident that the theoretical predictions overestimate the creep strengthening effect of whiskers. The factors responsible for this discrepancy rest on the assumption included in the shear-lag model that the short fibers (whiskers) have the uniform aspect ratio and are aligned along the load direction. In fact, some whiskers will inevitably be broken resulting in a whisker length distribution with an asymmetric character. At the same time, whisker misorientation also occurs during the extrusion process.

Considering the actual distribution of whiskers in the composites, two parameters,  $\chi_1$  and  $\chi_2$  are introduced to characterize the whisker length and orientation distribution, respectively, and they are defined as follows [49, 51, 82]

**Table 6** Theoretical and experimental load transfer coefficient for whiskers reinforced Al-Fe-V-Si composites ( $\alpha' = \chi_1 \chi_2 \alpha$ ).

$T$ (K)	SiCw/Al-Fe-V-Si			Al <sub>18</sub> B <sub>4</sub> O <sub>33</sub> w/Al-Fe-V-Si			Si <sub>3</sub> N <sub>4</sub> w/Al-Fe-V-Si	
	$\alpha$	$\alpha'$	$\beta$	$\alpha$	$\alpha'$	$\beta$	$\alpha$	$\alpha'$
573	0.456	0.296	0.350	0.452	0.294	0.369		
623	0.466	0.303	0.185	0.457	0.297	0.312		
673	0.462	0.300	0.234					
723	0.459	0.299	0.251	0.455	0.296	0.358		
773							0.451	0.293
823							0.445	0.289

$$\chi_1 = \int_0^{L_c} \left[ \frac{L^2}{2L_c L_m} \right] f(L) dL + \int_{L_c}^{\infty} \left( \frac{L}{L_m} \right) \left( 1 - \frac{L_c}{2L} \right) f(L) dL, \quad (8)$$

where  $L_c$  is the critical whisker length,  $L_m$  the mean whisker length and  $f(L)$  the two-parameter Weibull probability density function to describe the whisker length distribution and given by [83]

$$f(L) = mL^{n-1} \exp(-mL^n) \text{ for } L > 0, \quad (9)$$

where  $m$  and  $n$  are scale and shape parameters, respectively. Similarly, the whisker orientation coefficient  $\chi_2$  is expressed by [49, 51, 84, 85]

$$\chi_2 = 2 \int_{\theta_{\min}}^{\theta_{\max}} g(\theta) \cos^2(\theta) d\theta - 1, \quad (10)$$

where  $g(\theta)$  is the whisker orientation distribution function given as [82, 85]

$$g(\theta) = \frac{(\sin \theta)^{2p-1} (\cos \theta)^{2q-1}}{\int_{\theta_{\min}}^{\theta_{\max}} (\sin \theta)^{2p-1} (\cos \theta)^{2q-1} d\theta}, \quad (11)$$

where  $p$  and  $q$  are the shape parameters determining the shape of the distribution curves,  $0 \leq \theta_{\min} \leq \theta \leq \theta_{\max} \leq \pi/2$  and  $p \geq 1/2$  and  $q \geq 1/2$ . Then Eq. (6) can be modified as [49, 51]

$$\frac{\dot{\epsilon}_c}{\dot{\epsilon}_m} = \left[ \chi_1 \chi_2 \alpha \left( \frac{L}{d} \right)^{\frac{n+1}{n}} V_f + (1 - V_f) \right]^{-n}. \quad (12)$$

Based on the relevant geometric factors and the above equations, several effective strengthening factors of whiskers are presented in Table 7 and the modified load transfer coefficient,  $\alpha' = \chi_1 \chi_2 \alpha$  listed in Table 6. The experimental values of load transfer coefficient seem to vary with temperature while the shear-lag approaches do not consider the temperature dependence of load transfer. Incorporation of  $\chi_1 \chi_2 = 0.65$  into Eq. (12) yields an average ratio of  $\dot{\epsilon}_c / \dot{\epsilon}_m = 1.16 \times 10^{-2}$  for SiCw/Al-Fe-V-Si composites, which implies that at any selected (normalized) stress, the

**Table 7** The effective strengthening factors of whiskers [49, 51].

No.	$p$	$q$	$\chi_1 \chi_2$
1	0.5	1.0	0.228
2	1.0	4.0	0.415
3	1.0	8.0	0.540
4	1.0	16.0	0.609
5	0.5	10.0	0.630
6	4.0	100.0	0.637
7	0.5	16.0	0.650
8	0.5	32.0	0.671
9	1.0	100.0	0.678
10	0.5	100.0	0.685

(normalized) creep rate of the composite is lower than that of the matrix alloy by a factor of  $\sim 86$  and consistent with the experimental results (see Figure 11). The similar relations hold for the other two whisker reinforced composites.

By incorporating both a threshold stress and a modified load transfer coefficient, creep Eq. (3) for metal matrix composites is then re-written as [49, 50, 52]

$$\dot{\epsilon} = \frac{ADGb}{kT} \left[ \frac{(1 - \alpha')(\sigma - \sigma_{th})}{G} \right]^n \tag{13}$$

It follows from Eq. (13) that for a given value of  $(\sigma - \sigma_{th})$  and at the same temperature, the load transfer coefficient obtained experimentally,  $\beta$  is available through the expression

$$\beta = 1 - \left( \frac{\dot{\epsilon}_c}{\dot{\epsilon}_m} \right)^{1/n}, \tag{14}$$

where  $n$  is the true stress exponent with values of 5 and 8 for whisker-reinforced Al-Fe-V-Si and SiC/Al-C composites, respectively.

Figure 16 shows an example for comparison of the creep data between Al-Fe-V-Si alloy and SiCw/Al-Fe-V-Si composite plotted at a single temperature of 723 K in the logarithmic form of  $\dot{\epsilon}$  vs effective stress  $(\sigma - \sigma_{th})$ . The estimated values of  $\beta$  by means of this method for whisker-reinforced Al-Fe-V-Si and SiC/Al-C composites are summarized in Tables 6 and 8, respectively. It is instructive to note that the predicted

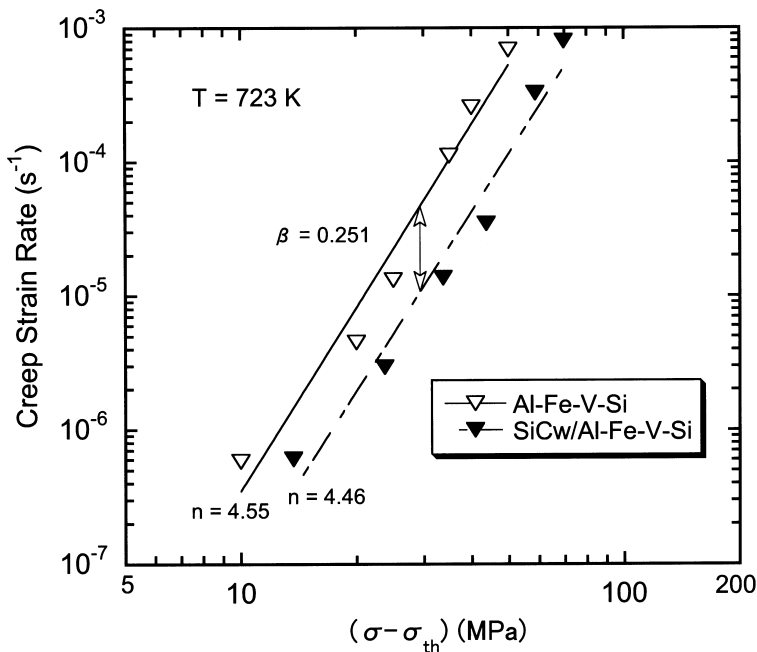


**Figure 16** Direct comparison on creep rate vs effective stress curve at 723 K determining the load transfer coefficient between Al-Fe-V-Si and SiCw/Al-Fe-V-Si.

**Table 8** The load transfer coefficient for SiC/AIC composites.

$T$ (K)	Experimental value		Predicted value*	
	SiC/AIC1	SiC/AIC2	SiC/AIC1	SiC/AIC2
623	0.638	0.507	0.460	0.468
723	0.432	0.416	0.467	0.474

\*Predicted by Eq. (7) using  $L/d = 1.0$  for particulates.

values of load transfer coefficient are in reasonable agreement with those obtained experimentally.

Further confirmation is provided in Figures 17 and 18 where the normalized creep rates for the matrix alloy and composites,  $\dot{\epsilon}/D_L$  are plotted against the apparent normalized effective stress  $(1 - \alpha')(\sigma - \sigma_{th})/G$  or  $(1 - \beta)(\sigma - \sigma_{th})/G$  ( $\alpha'$  and  $\beta$  are load transfer coefficient and both equal to zero for the matrix alloys). It

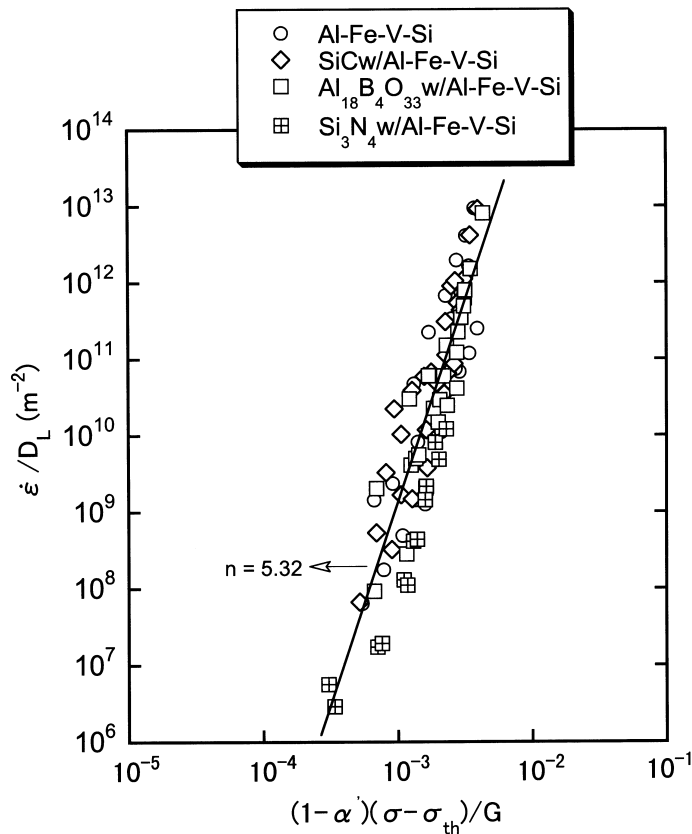
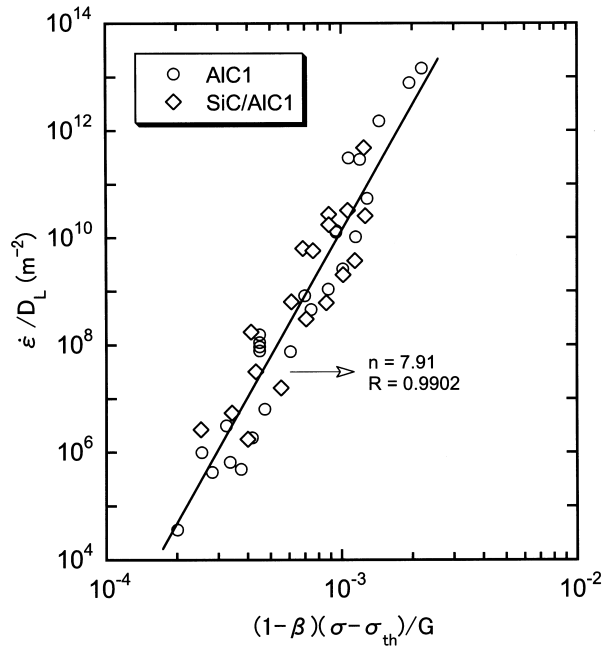
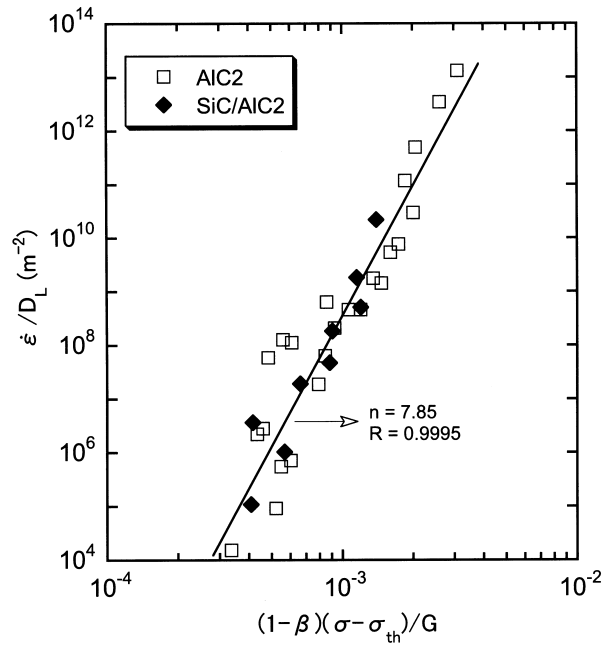


**Figure 17** Creep strain rates normalized with the lattice diffusion coefficient of aluminium,  $\dot{\epsilon}/D_L$  vs the apparent effective stress normalized with the shear modulus of aluminium,  $(1 - \alpha')(\sigma - \sigma_{th})/G$  for Al-Fe-V-Si and its whiskers reinforced composites ( $\alpha = 0$  for Al-Fe-V-Si matrix alloy).



(a)



(b)

**Figure 18** Creep strain rates normalized with the lattice diffusion coefficient of aluminium,  $\dot{\epsilon}/D_L$  vs the apparent effective stress normalized with the shear modulus of aluminium,  $(1-\beta)(\sigma-\sigma_{th})/G$  for (a) AIC1 and SiC/AIC1 and (b) AIC2 and SiC/AIC2 ( $\beta = 0$  for AIC matrix alloys).

follows from these figures that the normalized creep rates of the composites are very close to those of their corresponding matrix alloy.

In summary, as schematically depicted in Figure 19, dual scale dispersoids and ceramic reinforcements strengthening is an attractive means to improving the creep resistance of metals without changing the stress dependence of creep rates in composites. A creep strength parameter is defined by Rösler *et al.* to determine the combining strengthening effect as [43]

$$\Sigma = \sqrt{V_d} [1 + 2(2 + L/d)V_f^{3/2}], \quad (15)$$

where  $\Sigma$  is the creep strength parameter,  $V_d$  is the volume fraction of fine dispersoids present in the matrix alloy and other symbols have been defined previously. For moderate creep strength levels, it is noted that dispersion strengthening alone is insufficient since dispersoids are not capable of load transfer strengthening at high temperature in addition to their pinning effect on dislocation motion. However, combining ceramic reinforcements with realistic volume fractions can achieve satisfactory creep strength through load carrying capacity of reinforcements.

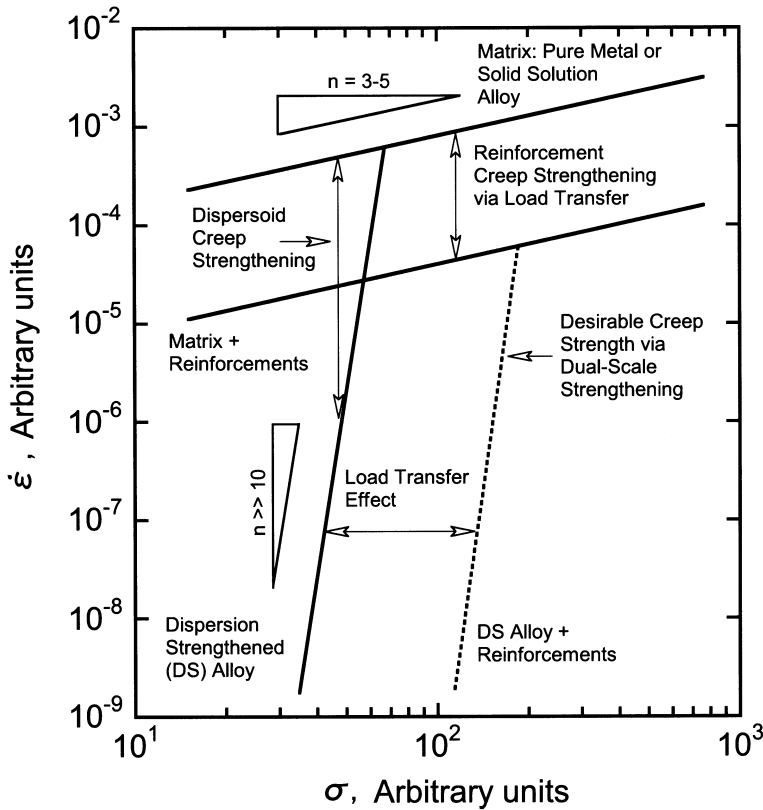


**Figure 19** Schematic illustration of steady-state creep rate vs applied stress for a typical dispersoid free matrix, dispersion strengthened (DS) material and ceramic reinforcement strengthened composite.

#### 4 Concluding remarks

The creep behavior in titanium matrix composites, two systems of DS aluminium alloys and their discontinuously reinforced composites was reviewed. The conclusions are drawn as follows.

- (1) In the discontinuous titanium matrix composites, there are two creep mechanisms: lattice-diffusion controlled dislocation climb ( $n = 4.3$ ) at low stresses, and pipe-diffusion controlled dislocation climb at high stresses. There is no threshold creep behavior as in the aluminium matrix composites. The creep strengthening in MMCs originates from combined effects of an increased modulus of the composites and the refined microstructures.
- (2) Analysis of the creep data of DS alloys and their composites indicates the presence of a threshold stress, that depends strongly on temperature. Available threshold stress models proposed for DS alloys cannot account for the temperature dependence of the threshold stress. A possible origin for the threshold stress in both the DS alloys and their composites is related to the interactions between dislocations and fine dispersoids in the matrix. Creep behavior in the composites and the unreinforced matrix alloy is controlled by the deformation in the matrix and the presence of ceramic reinforcements is not responsible for the source of the threshold stress. The threshold stress disappears at very high temperatures which means a transition of creep mechanism.
- (3) The addition of ceramic reinforcements to DS alloys results in enhancing the creep resistance of their matrix alloys over the entire range of strain rates. It is proposed that the creep strengthening is associated with the load transfer from the matrix to reinforcements, which can be described quantitatively based on the modified shear-lag approach where the effect of distribution for both length and orientation of reinforcements is taken into account. Therefore, dual-scale dispersoids and reinforcements strengthening is a promising means to achieve high creep resistance without change of the high stress sensitivity of creep rate.
- (4) When a threshold stress and the contribution of load transfer are incorporated into the analysis, the creep rate for composites can be described by the equation

$$\dot{\epsilon} = \frac{ADGb}{kT} \left[ \frac{(1 - \alpha)(\sigma - \sigma_{th})}{G} \right]^n$$

where  $\alpha$  is the load transfer coefficient. One of the effective ways for development of creep-resistant MMCs is to combine the nano-sized particles and micro-sized reinforcements.

- (5) It is noted that creep fracture of MMCs has not been well studied compared to creep deformation. The creep damage mechanism and creep life prediction method have not been established. These need to be investigated in the future.

#### 5 Outlook

Although there have been a lot of applications of discontinuous MMCs in automotive and aerospace industries, a number of technological barriers, such as

low fracture toughness, high cost of raw materials and machining for components, exist for widespread applications. Moreover, the data bank of mechanical properties is not enough for designers to evaluate how to balance the performance and cost.

Several new trends for development are noteworthy of mentioning as follows:

- Functionally gradient metal matrix composites (FGMMCs) appeared and are being studied. FGMMCs are the same idea as functional gradient materials with continuous change in composition and/or microstructure. Accordingly, FGMMCs have become attractive and have the potential to be utilized in a wide range of engineering applications, such as advanced engines, armor, medical implants, and electronic devices [86, 87]. The main advantages of the compositionally graded composites are the gradual change of properties such as coefficient of heat conductivity and electrical conductivity, thermal stress, etc. [88, 89]. The concept of FGMMCs has also been applied in protective coatings in metal matrix composites [90].
- The laminated approach [91–96] has been identified as a promising technique to improve the toughness of discontinuously reinforced metal matrix composites, where delamination along the interface is considered as a mechanism for crack blunting and the spreading of deformation. The level of improvement is dependent on the test orientation [95].
- In order to meet specific requirements, such as high flexural strength, high stiffness, and wear-resistance, or a low coefficient of thermal expansion, MMCs with high volume fraction of reinforcements up to 50% are being developed [97–99]. High-pressure [98–102] or pressureless [103] infiltration and squeeze-cast [104, 105] have been considered as a promising process to fabricate these composites using ceramic preforms. By using these two techniques, the distribution of reinforcements is quite uniform. Elimination of residual porosities and absence of interfacial reactions between the reinforcements and the matrix can be ensured in the final products. Furthermore, the resulting properties of MMCs can be adjusted to the required values via additions of appropriate additional alloying elements. Additionally, when suitable barriers are used to prevent the infiltration of molten metal it is also possible to fabricate net- or near-net-shaped MMCs.
- The magnesium alloys and their matrix composites are now hot topics due to their high specific properties. Since a high reactivity between the magnesium and the reinforcement results in better interfaces than by using an aluminium alloy matrix, much work has already been done on reinforcing magnesium with graphite fibers, SiC particulates and whiskers, Al<sub>2</sub>O<sub>3</sub> fibers and particulates [106]. However, in several magnesium matrix-reinforcement combinations, this reactivity leads to limitations in elevated temperature applications due to severe interfacial reactions. For example, in contrast to aluminium matrices, magnesium and magnesium alloys show excellent wetting with Al<sub>2</sub>O<sub>3</sub>. From the thermodynamical point of view, Al<sub>2</sub>O<sub>3</sub> is not stable against chemical reaction with magnesium, resulting in the formation of an MgAl<sub>2</sub>O<sub>4</sub> spinel or MgO. Therefore some approaches, such as the modification of the matrix composition, coating of the reinforcement, specific treatments to the reinforcement and control of process parameters are proposed to obtain desired interfaces with better properties [90].

- The recycling technology of MMCs is a very important subject. This difficulty is also an obstacle for the wide applications of MMCs, although research on the recycling is going on. It is noted that the research on performance should be emphasized in the future, compared to attempting high values of some mechanical properties only at present.

### Acknowledgements

One of the authors (L. M. Peng) greatly appreciates the Research Fellowship awarded by Science and Technology Agency (STA), Japan. The authors are very grateful to Prof. J. Cadek for his advice and encouragement on our research.

### References

- 1 Zhu, S. J., Lu, Y. X., Wang, Z. G. and Bi, J. (1992) 'Creep behavior of TiC-particulate-reinforced Ti alloy composite', *Mater. Lett.*, 13(4–5), 199–203.
- 2 Zhu, S. J., Lu, Y. X., Wang, Z. G. and Bi, J. (1992) 'Cyclic creep behavior of TiC(particulate)/Ti-6Al-4V composites in the temperature range of  $0.4-0.5T_m$ ', *J. Mater. Sci. Lett.*, 11(10), 630–632.
- 3 Zhu, S. J., Lu, Y. X., Wang, Z. G. and Bi, J. (1993) *Metal Matrix Composites*, Miravete, A. (Ed.), London: Woodhead, pp. 549–556.
- 4 Ranganath, S. and Mishra, R. S. (1996) 'Steady-state creep behavior of particulate-reinforced titanium matrix composites', *Acta Mater.*, 44(3), 927–935.
- 5 Tsang, H. T., Chao, C. G. and Ma, C. Y. (1997) 'Effects of volume fraction of reinforcement on tensile and creep properties of in-situ TiB/Ti MMC', *Scripta Mater.*, 37(9), 1359–1365.
- 6 Ranganath, S. (1997) 'A review on particulate-reinforced titanium matrix composites', *J. Mater. Sci.*, 32(1), 1–16.
- 7 Zhu, S. J., Mukherji, D., Chen, W., Lu, Y. X., Wang, Z. G. and Wahi, R. P. (1998) 'Steady-state creep behavior of TiC particulate reinforced Ti-6Al-4V composite', *Mater. Sci. Eng.*, A256, 301–307.
- 8 Zhu, J. H., Liaw, P. K., Corum, J. M. and McCoy, H. E. (1999) 'High-temperature mechanical behavior of Ti-6Al-4V alloy and TiCp/Ti-6Al-4V composite', *Metall. Mater. Trans.*, 30A(7), 1569–1578.
- 9 Nieh, T. G. (1984) 'Creep rupture of a silicon carbide reinforced aluminium composite', *Metall. Trans.*, 15A(1), 139–146.
- 10 Nardone, V. C. and Strife, J. R. (1987) 'Analysis of the creep behavior of silicon carbide whisker reinforced 2124 Al (T4)', *Metall. Trans.*, 18A(1), 109–114.
- 11 Morimoto, T., Yamaoka, T., Lillholt, H. and Taya, M. (1988) 'Second stage creep of SiC whisker/6061 aluminium composite at 573 K', *J. Eng. Mater. Tech.*, 110(1), 70–76.
- 12 Nieh, T. G., Xia, K. and Langdon, T. G. (1988) 'Mechanical properties of discontinuous SiC reinforced aluminium composite at elevated temperatures', *J. Eng. Mater. Tech.*, 110(1), 77–82.
- 13 Mishra, R. S. and Pandey, A. B. (1990) 'Some observations on the high-temperature creep behavior of 6061 Al-SiC composites', *Metall. Trans.*, 21A(8), 2089–2090.
- 14 Pandey, A. B., Mishra, R. S. and Mahajan, Y. R. (1990) 'Creep behavior of an aluminium-silicon carbide particulate composite', *Scripta Metall.*, 24(10), 1565–1570.

- 15 Dragone, T. L. and Nix, W. D. (1990) 'Geometric factors affecting the internal stress distribution and high temperature creep of discontinuous fiber reinforced metals', *Acta Metall. Mater.*, 38(10), 1941–1953.
- 16 Park, K. T., Lavernia, E. J. and Mohamed, F. A. (1990) 'High temperature creep of silicon carbide reinforced aluminium', *Acta Metall. Mater.*, 38(11), 2149–2159.
- 17 Mohamed, F. A., Park, K. T. and Lavernia, E. J. (1992) 'Creep behavior of discontinuous SiC-Al composites', *Mater. Sci. Eng.*, 150A, 21–35.
- 18 Dragone, T. L. and Nix, W. D. (1992) 'Steady state and transient creep properties of an aluminium alloy reinforced with alumina fibers', *Acta Metall. Mater.*, 40(10), 2781–2791.
- 19 Pandey, A. B., Mishra, R. S. and Mahajan, Y. R. (1992) 'Steady-state creep behavior of silicon carbide particulate reinforced aluminium composites', *Acta Metall. Mater.*, 40(8), 2045–2052.
- 20 Gonzalez-Doncel, G. and Sherby, O. D. (1993) 'High temperature creep behavior of metal matrix aluminium-SiC composites', *Acta Metall. Mater.*, 41(10), 2797–2805.
- 21 Krajewski, P. E., Allison, J. E. and Jones, J. W. (1993) 'The influence of matrix microstructure and particulate reinforcement on the creep behavior of 2219 aluminium', *Metall. Trans.*, 24A(10), 2731–2741.
- 22 Cadek, J., Sustek, V. and Pahutova, M. (1994) 'Is creep in discontinuous metal matrix composites lattice diffusion controlled?' *Mater. Sci. Eng.*, A174, 141–147.
- 23 Cadek, J., Oikawa, H. and Sustek, V. (1995) 'Threshold creep behavior of discontinuous aluminium and aluminium alloy matrix composites', *Mater. Sci. Eng.*, A190, 9–23.
- 24 Park, K. T. and Mohamed, F. A. (1995) 'Creep strengthening in a discontinuous SiC-Al composite', *Metall. Mater. Trans.*, 26A(12), 3119–3129.
- 25 Pandey, A. B., Mishra, R. S. and Mahajan, Y. R. (1996) 'Effect of a solid solution on the steady-state creep behavior of an aluminium matrix composite', *Metall. Mater. Trans.*, 27A(2), 305–316.
- 26 Li, Y. and Mohamed, F. A. (1997) 'An investigation of creep behavior in a SiC-2124 Al composite', *Acta Mater.*, 45(11), 4775–4785.
- 27 Li, Y. and Langdon, T. G. (1997) 'Creep behavior of an Al-6061 metal matrix composite reinforced with alumina particulates', *Acta Mater.*, 45(11), 4797–4806.
- 28 Li, Y. and Langdon, T. G. (1998) 'Creep behavior of a reinforced Al-7075 alloy: implications for the creep processes in metal matrix composites', *Acta Mater.*, 46(4), 1143–1155.
- 29 Li, Y. and Langdon, T. G. (1998) 'A comparison of the creep properties of an Al-6092 composite and the unreinforced alloy', *Metall. Mater. Trans.*, 29A(10), 2523–2531.
- 30 Li, Y. and Langdon, T. G. (1999) 'A unified interpretation of threshold stresses in the creep and high strain rate superplasticity of metal matrix composites', *Acta Mater.*, 47(12), 3395–3403.
- 31 Ma, Z. Y. and Tjong, S. C. (1999) 'The high temperature creep behavior of 2124 aluminium alloys with and without particulate and SiC-whisker reinforcement', *Comp. Sci. Tech.*, 59(5), 737–747.
- 32 Li, Y. and Langdon, T. G. (1999) 'Fundamental aspects of creep in metal matrix composites', *Metall. Mater. Trans.*, 30A(2), 315–324.
- 33 Wakashima, K., Moriyama T. and Mori, T. (2000) 'Steady-state creep of a particulate SiC/6061 Al composite', *Acta Mater.*, 48(3), 891–901.
- 34 Ma, Z. Y. and Tjong, S. C. (2001) 'Creep deformation characteristics of discontinuously reinforced aluminium-matrix composites', *Comp. Sci. Tech.*, 61(5), 787–795.
- 35 Rösler, J., Valencia, J. J., Levi, C. G., Evans, A. G. and Mehrabian, R. (1990) 'Intermetallic matrix composites', *Mater. Res. Soc. Sym. Proc.*, 194, 241–248.

- 36 Kampe, S. L., Bryant, J. D. and Christodoulou, L. (1991) 'Creep deformation of TiB<sub>2</sub>-reinforced near- $\gamma$  titanium aluminides', *Metall. Trans.*, 22A(2), 447–454.
- 37 Froes, F. H., Yau, T. L. and Weidinger, H. G. (1996) *Materials Science and Technology*, Cahn, R. W., Haasen, P. and Kramer, E. J. (Eds), Weinheim, Germany: VCH Verlagsgesellschaft mbH, pp. 405–408.
- 38 Frost, H. J. and Ashby, M. F. (1982) *Deformation–Mechanism Maps*, Pergamon Press, p. 44.
- 39 Malkondaiah, G. and Rao, P. R. (1981) 'Creep of alpha-titanium at low stresses', *Acta Metal.*, 29(6), 1263–1275.
- 40 Eylon, D., Hall, J. A., Pierce, C. M. and Ruckle, D. L. (1976) 'Microstructure and mechanical properties relationship in the Ti-11 alloy at room and elevated temperatures', *Metall. Trans.*, 7A(7), 1817–1826.
- 41 Rösler, J. and Arzt, E. (1990) 'A new model-based creep equation for dispersion strengthened materials', *Acta Metal. Mater.*, 38(4), 671–683.
- 42 Jansen, A. M. and Dunand, D. C. (1997) 'Creep of metals containing high volume fraction of unshearable dispersoids—Part II. Experiments in the Al-Al<sub>2</sub>O<sub>3</sub> system and comparison to models', *Acta Mater.*, 45(11), 4583–4592.
- 43 Rösler, J. and Bäker, M. (2000) 'A theoretical concept for the design of high-temperature materials by dual-scale particle strengthening', *Acta Mater.*, 48(13), 3553–3567.
- 44 Peng, L. M., Zhu, S. J., Ma, Z. Y., Bi, J., Chen, H. R. and Wang, F. G. (1998) 'High temperature creep deformation of Al-Fe-V-Si alloy', *Mater. Sci. Eng.*, A259, 25–33.
- 45 Cadek, J., Kucharová, K. and Zhu, S. J. (2002) 'Creep behaviour of an Al-8.5Fe-1.3V-1.7Si-15SiCp composite at temperatures ranging from 873 to 948 K', *Mater. Sci. Eng.*, A328, 283–290.
- 46 Ma, Z. Y., Pan, J., Ning, X. G., Li, J. H., Lu, Y. X. and Bi, J. (1994) 'Aluminium borate whisker reinforced Al-8.5Fe-1.3V-1.7Si composite', *J. Mater. Sci. Lett.*, 13(24), 1731–1732.
- 47 Kim, I. S., Kim, N. J. and Nam, S. W. (1995) 'Temperature dependence of the optimum particle size for the dislocation detachment controlled creep of Al-Fe-V-Si/SiCp composite', *Scripta Metall. Mater.*, 32(11), 1813–1819.
- 48 Zhu, S. J., Peng, L. M., Ma, Z. Y., Bi, J., Wang, F. G. and Wang, Z. G. (1996) 'High temperature creep behavior of SiC whisker-reinforced Al-Fe-V-Si composite', *Mater. Sci. Eng.*, A215, 120–124.
- 49 Peng, L. M., Zhu, S. J., Ma, Z. Y., Bi, J., Chen, H. R. and Wang, F. G. (1998) 'Examination on compression creep behavior of an Al-Fe-V-Si alloy and SiC whisker reinforced Al-Fe-V-Si composite', *J. Mater. Sci.*, 33(23), 5643–5652.
- 50 Peng, L. M., Zhu, S. J., Ma, Z. Y., Bi, J., Chen, H. R. and Wang, F. G. (1999) 'The effect of Si<sub>3</sub>N<sub>4</sub> whiskers on the high temperature creep behavior of an Al-Fe-V-Si alloy matrix composite', *Comp. Sci. Tech.*, 59(5), 769–773.
- 51 Peng, L. M., Zhu, S. J., Ma, Z. Y., Bi, J., Wang, F. G., Chen, H. R. and Northwood, D. O. (1999) 'High temperature creep deformation of Al<sub>18</sub>B<sub>4</sub>O<sub>33</sub> whiskers reinforced 8009 Al composite', *Mater. Sci. Eng.*, A265, 63–70.
- 52 Zhu, S. J., Peng, L. M., Zhou, Q., Ma, Z. Y., Kucharová, K. and Cadek, J. (2000) 'Creep behavior of an aluminium strengthened by fine aluminium carbide particles and reinforced by silicon carbide particulates-DS Al-SiC/Al<sub>4</sub>C<sub>3</sub> composites', *Mater. Sci. Eng.*, A282, 273–284.
- 53 Zhou, Q., Zhu, S. J., Ma, Z. Y., Zhao, J. and Bi, J. (1998) 'Creep of SiC particulates reinforced Al-C-O composites', *J. Mater. Sci.*, 33(13), 3433–3436.
- 54 Cadek, J., Zhu, S. J. and Milicka, K. (1998) 'Creep behavior of ODS aluminium reinforced by silicon carbide particulates-an ODS Al-30SiCp composite', *Mater. Sci. Eng.*, A248, 65–72.

- 55 Cadek, J., Kucharová, K. and Zhu, S. J. (1999) 'Creep behavior of an oxide dispersion strengthened Al-5Mg alloy reinforced by silicon carbide particulates-an oxide dispersion strengthened Al-5Mg-30SiCp composite', *Mater. Sci. Eng.*, A272, 45–56.
- 56 Cadek, J., Kucharová, K. and Zhu, S. J. (2000) 'High temperature creep behavior of an Al-8.5Fe-1.3V-1.7Si alloy reinforced with silicon carbide particulates', *Mater. Sci. Eng.*, A283, 172–180.
- 57 Mitra, S. (1996) 'Elevated temperature deformation behavior of a dispersion-strengthened Al-Fe, V, Si alloy', *Metall. Mater. Trans.*, 27A(12), 3913–3923.
- 58 Carreño, F. and Ruano, O. A. (1998) 'Separated contribution of particles and matrix on the creep behavior of dispersion strengthened materials', *Acta Mater.*, 46(1), 159–167.
- 59 Zhu, S. J., Kucharová, K. and Cadek, J. (2000) 'High temperature creep in an Al-8.5Fe-1.3V-1.7Si alloy processed by rapid solidification', *Metall. Mater. Trans.*, 31A(9), 2229–2237.
- 60 Park, K. T., Lavernia, E. J. and Mohamed, F. A. (1994) 'High temperature deformation of 6061 Al', *Acta Metall.*, 42(3), 667–678.
- 61 Li, Y., Nutt, S. R. and Mohamed, F. A. (1997) 'An investigation of creep and substructure formation in 2124 Al', *Acta Mater.*, 45(6), 2607–2620.
- 62 Lundy, T. S. and Murdock, J. F. (1962) 'Diffusion of Al<sup>26</sup> and Mn<sup>54</sup> in aluminium', *J. Appl. Phys.*, 33(5), 1671–1673.
- 63 Bird, J. E., Mukherjee, A. K. and Dorn, J. E. (1969) *Quantitative Relations Between Properties and Microstructures*, Branbon, D. G. and Rosen, A. (Eds), Jerusalem: Israel University Press, p. 225.
- 64 Weertman, J. (1957) 'Steady-state creep of crystals', *J. Appl. Phys.*, 28(3), 1185–1189.
- 65 Mohamed, F. A. and Langdon, T. G. (1974) 'The transition from dislocation climb to viscous glide in creep of solid solution alloys', *Acta Metall. Mater.*, 22(3), 779–788.
- 66 Weertman, J. (1957) 'Steady-state creep through dislocation climb', *J. Appl. Phys.*, 28(1), 362–364.
- 67 Sherby, O. D., Klundt, R. H. and Miller, A. K. (1977) 'Flow stress, subgrain size, and subgrain stability at elevated temperature', *Metall. Trans.*, 8A(4), 843–850.
- 68 Orowan, E. (1954) *Dislocations in Metals*, Cohen, M. (Ed.), New York: AIME, p. 1954.
- 69 Kocks, U. F. (1966) 'A statistical theory of flow stress and work-hardening', *Phil. Mag.*, 13(3), 541–566.
- 70 Shewfelt, R. S. W. and Brown, L. M. (1977) 'High-temperature strength of dispersion-hardened single crystals, II', *Theory, Phil. Mag.*, 35(6), 945–962.
- 71 Arzt, E. and Ashby, M. F. (1982) 'Threshold stresses in materials containing dispersed particles', *Scripta Metall.*, 16(11), 1285–1290.
- 72 Arzt, E. and Wilkinson, D. S. (1986) 'Threshold stresses for dislocation climb over hard particles: the effect of an attractive interactions', *Acta Metall.*, 34(7), 1893–1898.
- 73 Arzt, E. and Rösler, J. (1988) 'The kinetics of dislocation climb over hard particles—II effect of an attractive particle-dislocation interactions', *Acta Metall.*, 36(4), 1053–1060.
- 74 Friedel, J. (1964) *Dislocations*, Chapt. 16, Oxford.
- 75 Cadek, J., Kucharova, K. and Zhu, S. J. (2001) 'Threshold creep behavior of an Al-8.5Fe-1.3V-1.7Si alloy reinforced with silicon carbide particulates', *Kovove Mater.*, 39(1), 77–84.
- 76 Cadek, J., Kucharova, K. and Sustek, V. (1999) 'A PM 2124 Al-20SiCp composite: disappearance of true threshold creep behavior at high testing temperatures', *Scripta Mater.*, 40(11), 1269–1275.
- 77 Mishra, R. S., Nandy, T. K. and Greenwood, G. W. (1994) 'The threshold stress for creep controlled by dislocation-particle interactions', *Phil. Mag.*, A69(5), 1097–1109.

- 78 Kloc, L., Spigarelli, S., Cerri, E., Evangelista, E. and Langdon, T. G. (1996) 'An evaluation of the creep properties of two Al-Si alloys produced by rapid solidification processing', *Metall. Mater. Trans.*, 27A(12), 3871–3879.
- 79 Yavari, P., Mohamed, F. A. and Langdon, T. G. (1981) 'Creep and substructure formation in an Al-5%Mg solid solution alloy', *Acta Metall.*, 29(7), 1495–1507.
- 80 Yavari, P. and Langdon, T. G. (1982) 'An examination of the breakdown in creep by viscous glide in solid solution alloys at high stress levels', *Acta Metall.*, 30(12), 2181–2196.
- 81 Kelly, A. and Street, K. N. (1972) 'Creep of discontinuous fiber composites II, theory for the steady-state', *Proc. R. Soc. Lon.*, A328(2), 283–293.
- 82 Fu, S. Y. and Lauke, B. (1996) 'Effect of fiber length and fiber orientation distribution on the tensile strength of short-fiber-reinforced polymers', *Comp. Sci. Tech.*, 56(8), 1179–1190.
- 83 Ulrych, F., Sova, M., Vokrouhlecky, J. and Turcic, B. (1993) 'Empirical relations of the mechanical properties of polyamide 6 reinforced with short glass fibers', *Polym. Comp.*, 14(2), 229–237.
- 84 Chiang, C. R. (1994) 'A statistical theory of the tensile strength of short fiber-reinforced composites', *Comp. Sci. Tech.*, 50(3), 479–482.
- 85 Fu, S. Y. and Lauke, B. (1998) 'The elastic modulus of misaligned short-fiber-reinforced polymers', *Comp. Sci. Tech.*, 58(3), 389–400.
- 86 Zhu, S. J., Xu, F. M. and Wang, F. G. (2002) 'Fabrication and fatigue crack growth behaviour of SiC/Al graded metal matrix composite', *Proc. Ann. Conf. Metals*, Japan Institute of Metals, Tokyo, p. 480.
- 87 Koizumi, M. (1992) *Proc. 16th Ann. Conf. Composites and Adv. Ceram. Mater.*, The American Ceramic Society, Westerville, OH, pp. 333–347.
- 88 Ho, S. and Lavernia, E. J. (1996) 'Thermal residual stresses in functionally graded and layered 6061 Al/SiC materials', *Metall. Mater. Trans.*, 27A(10), 3241–3249.
- 89 Liu, Q. M., Jiao, Y. N., Yang, Y. S. and Hu, Z. Q. (1996) 'Theoretical analysis of the particle gradient distribution in centrifugal field during solidification', *Metall. Mater. Trans.*, 27B(6), 1025–1029.
- 90 Rajan, T. P. D., Pillai, R. M. and Pai, B. C. (1998) 'Reinforcement coatings and interfaces in aluminium matrix composites (Review)', *J. Mater. Sci.*, 33(14), 3491–3503.
- 91 Leng, Y. and Courtney, T. C. (1990) 'Fracture behavior of laminated metal-metallic glass composites', *Metall. Trans.*, 21A(8), 2159–2168.
- 92 Ellis, L. Y. and Lewandowski, J. J. (1991) 'Laminated composites with improved bending ductility and toughness', *J. Mater. Sci. Lett.*, 10(5), 461–463.
- 93 Lee, S., Wadsworth, J. and Sherby, O. D. (1991) 'Tensile properties of laminated composites based on ultrahigh carbon steel', *J. Comp. Mater.*, 25(5), 842–853.
- 94 Nardone, V. C., Strife, J. R. and Prewo, K. M. (1991) 'Microstructurally toughened particulate-reinforced aluminium matrix composites', *Metall. Trans.*, 22A(1), 171–182.
- 95 Zhang, J. and Lewandowski, J. J. (1997) 'Delamination study using four-point bending of bilayers', *J. Mater. Sci.*, 32(15), 3851–3856.
- 96 Pandey, A. B., Majumdar, B. S. and Miracle, D. B. (2001) 'Laminated particulate-reinforced aluminum composites with improved toughness', *Acta Mater.*, 49, 405–417.
- 97 Nagendra, N. and Jayaram, V. (2000) 'Fracture and R-curves in high volume fraction of Al<sub>2</sub>O<sub>3</sub>/Al composites', *J. Mater. Res.*, 15(5), 1131–1144.
- 98 Chen, C. Y. and Chao, C. G. (2000) 'Effect of particle-size distribution on the properties of high-volume-fraction SiCp-Al-based composites', *Metall. Mater. Trans.*, 31A(9), 2351–2359.

- 99 Kouzeli, M., Weber, L., San Marchi, C. and Mortensen, A. (2001) 'Quantification of microdamage phenomena during tensile straining of high volume fraction particle reinforced aluminium', *Acta Mater.*, 49, 497–505.
- 100 Peng, L. M., Noda, K. and Kawamoto, H. (2001) 'Microstructure and mechanical properties of high-pressure cast Si<sub>3</sub>N<sub>4</sub>/Al composites', *Proc. Ann. Conf. Ceram.*, The Ceramic Society of Japan, Tokyo, p. 5.
- 101 Ibrahim, A., Mohamed, F. A. and Lavernia, E. J. (1991) 'Particulates reinforced metal matrix composites—a review', *J. Mater. Sci.*, 26(5), 1137–1156.
- 102 Biswas, D. K., Gatica, J. E. and Tewari, S. N. (1998) 'Dynamic analysis of unidirectional pressure infiltration of porous preforms by pure metals', *Metall. Mater. Trans.*, 29A(1), 377–385.
- 103 Candan, E., Atkinson, H. V. and Jones, H. (2000) 'Effect of ceramic particle size and applied pressure on time to complete infiltration of liquid aluminium into SiC powder compacts', *J. Mater. Sci.*, 35(21), 4955–4960.
- 104 Lee, K. B., Kim, Y. S. and Kwon, H. (1998) 'Fabrication of Al-3 wt pct Mg matrix composites reinforced with Al<sub>2</sub>O<sub>3</sub> and SiC particulates by the pressureless infiltration technique', *Metall. Mater. Trans.*, 29A(12), 3087–3095.
- 105 Lee, J. C., Kim, G. H., Lee, J. I. and Lee, H. I. (1997) 'Interfacial reactions in the squeeze-cast (SAFFIL + C)/SAE 329 Al composites', *Metall. Trans.*, 28A(5), 1251–1259.
- 106 Sohn, K. S., Euh, K., Lee, S. and Park, I. (1998) 'Mechanical properties and fracture behavior of squeeze-cast Mg matrix composites', *Metall. Trans.*, 29A(10), 2543–2554.
- 107 Neite, G., Kubota, K., Higashi, K. and Hehmann, F. (1996) *Materials Science and Technology*, Cahn, R. W., Haasen, P. and Kramer, E. J. (Eds), Weinheim, Germany, Vol. 8, pp. 198–201.